Red Balloon Rock Shelter: Iron Age and Middle Stone Age occupations on the Waterberg Plateau in Limpopo, South Africa

Lyn Wadley, Guilhem Mauran, Christine Sievers, Hennie van Deventer, Wim Biemond, Klaas Seanego, Bo Li, Zenobia Jacobs

Southern African Humanities **34**: 19–58 September 2021 KwaZulu-Natal Museum

Red Balloon Rock Shelter: Iron Age and Middle Stone Age occupations on the Waterberg Plateau in Limpopo, South Africa

[1]**Lyn Wadley**, [1]**Guilhem Mauran**, [2]**Christine Sievers**, [3]**Hennie van Deventer**, [3]**Wim Biemond**, [4]**Klaas Seanego**, [5,6]**Bo Li** and [5,6]**Zenobia Jacobs**

[1]Evolutionary Studies Institute, University of the Witwatersrand, Johannesburg, South Africa; lyn.wadley@wits.ac.za; guilhem.mauran@mnhn.fr

[2]School of Geography, Archaeology and Environmental Studies, University of the Witwatersrand, Johannesburg, South Africa; christine.sievers@wits.ac.za

[3]Anthropology and Archaeology Department, University of South Africa; biemondwm@gmail.com; hennievd@lantic.net

[4] Reserve on which Red Balloon Rock Shelter is situated

[5]Centre for Archaeological Science, School of Earth, Atmospheric and Life Sciences, University of Wollongong, Australia; bli@uow.edu.au; zenobia@uow.edu.au

[6]Australian Research Council Centre of Excellence for Australian Biodiversity and Heritage, University of Wollongong, Australia; bli@uow.edu.au; zenobia@uow.edu.au

ABSTRACT

Red Balloon Rock Shelter is located at 1 200 m above mean sea level on the Waterberg Plateau, Limpopo Province. The surface of the deep, dry shelter is strewn with Iron Age ceramics of many facies, and Middle Stone Age (MSA) lithics. It may have been used as a rain-making site from the time of the first Iron Age settlement in the area. In addition to ceramics, there are many ostrich eggshell beads, some worked bone, and seeds that imply vegetation similar to the current vegetation, and the possible use of red balloon (*Erythrophysa transvaalensis*) seeds as beads. There was, however, probably no agropastoralist occupation within the shelter until the *difaqane* or just before it. A single preliminary date of 250±80 BP on charcoal from a large hearth supports an interpretation of the shelter as a Tswana rain-control site. The long hiatus between this refugium and the MSA occupation is not geologically marked. The shelter was first inhabited by people close to 100 000 years ago when stone tool-makers were using Levallois, blade, and bipolar flaking for a variety of lithic products that included scrapers, denticulates, points, and backed tools. The lithics were coated in dried mud, suggesting that a wetter than present phase followed the last of the MSA occupations in the shelter.

KEY WORDS: Waterberg, Iron Age refuge, rain-making, ceramics, Middle Stone Age, lithics, Marine Isotope Stage 5.

The earliest archaeological remains in Limpopo Province (Limpopo) are from the Makapan Valley near Mokopane (formerly Potgietersrus). Here, remains of *Australopithecus africanus* in the Limeworks site, and the long Stone Age sequence at Cave of Hearths (Mason 1962, 1988; Sampson 1974; Sinclair 2009), have contributed to the Valley's inclusion in the Cradle of Humankind World Heritage Site. Limpopo boasts a second World Heritage Site at Mapungubwe on the Limpopo River where there is evidence for South Africa's earliest (AD 1220–1300) state headed by a king (Huffman 2007). While best known for its Iron Age golden treasures (Huffman 2007), exotic glass beads (Wood 2011) and hilltop rain-making sites (Schoeman 2006), the Mapungubwe area also has a wealth of Earlier (ESA), Middle (MSA) and Later Stone Age (LSA) sites (Van Doornum 2008; Wilkins 2008; Pollarolo & Kuman 2009; Le Baron et al. 2010; Sumner 2013; Forssman 2020).

ISSN 2305-2791 (online); 1681-5564 (print)

Fig. 1. Approximate location of Red Balloon Rock Shelter in Limpopo Province. Some Limpopo Middle Stone Age sites are included with names abbreviated: Red Balloon Rock Shelter, Olieboomspoort Rock Shelter, Bushman Rock Shelter, North Brabant Rock Shelter and Mwulu's Cave. Kalkbank, Steenbokfontein, Wonderkrater and Blaaubank are open sites.

The Stone Age background

Archaeological interest in the Stone Age of Limpopo has waxed and waned over the past 80 years. Early on, Mason (1962) recorded at least 61 MSA sites (which he classified as Pietersburg Industries) in the northern part of South Africa (formerly known as the Transvaal). He and other luminaries like C. (Peter) van Riet Lowe, James Kitching, Raymond Dart, Robert Broom, and Philip Tobias excavated some of these northernmost Stone Age sites in the first flush of interest here (Goodwin & Van Riet Lowe 1929; Tobias 1949; Mason 1951, 1957). Then, for about 50 years, more attention was lavished on Stone Age sites in the Cape, particularly those at the coast. A resurgence of interest in Limpopo's Stone Age began with new excavations such as those in the Makapan Valley (Sinclair 2009), the Limpopo Valley (Kuman et al. 2005), Olieboomspoort (Van der Ryst 2006; Val et al. 2021), Wonderkrater (Backwell et al. 2014) (Fig. 1) and the Waterberg plateau (Van der Ryst 1998).

Before discussing the Stone Age on the Waterberg plateau where Red Balloon Rock Shelter is situated, we provide some background to Limpopo sites below the escarpment. Makapan Valley seems the best place to start, not least because of the Herculean task undertaken at Cave of Hearths (Fig. 1), where heavily cemented sediments were detonated with dynamite from the cliff face by Mason, who had to acquire a blasting licence for the task. Here, in the youngest ESA occupations of

Bed 3, the mandible of a hominid thought to be a precursor of *Homo sapiens* was recovered (Tobias 1971). Although no dates are available for Cave of Hearths, Bed 3 is thought to be about 300 000 years (300 ka) old and this would be chronologically consistent with final ESA/early MSA elsewhere in Africa (Hublin et al. 2017). Ancient *H. sapiens* skeletons are rare in Stone Age sites in Limpopo, though one recovered from Tuinplaats on the Springbok Flats was dated by uranium series on bone to possibly 20 ka ago and possibly as young as 11 ka ago (Pike et al. 2004). Beds 4–9 from Cave of Hearths yielded MSA lithics with many blades and unifacial points (Mason 1962; Sinclair 2009).

From the 1950s onwards, archaeologists excavating MSA sites in the interior of South Africa named stone tool industries with long blades and long unifacial points after the town of Pietersburg (now Polokwane). More recently, Paloma de la Peña and colleagues (2018) have argued that Pietersburg industries have no technological or even typological coherence, and are a 'catch-all' for MSA assemblages in northernmost South Africa. While the best-known Stone Age site in Limpopo is Cave of Hearths, there are other important ones like Mwulu's Cave not far from the Makapan Valley (Tobias 1949; Sampson 1974), Olieboomspoort near Lephalale (Mason 1962; Van der Ryst 2006), and, to the far eastern border of the province, Bushman Rock Shelter near Ohrigstad (Plug 1981; Porraz et al. 2015). Olieboomspoort has MSA assemblages made from a variety of fine-grained rocks, and they overlie an ESA assemblage and underlie a long LSA sequence (Mason 1962; Van der Ryst 2006). Only a handful of Stone Age sites in South Africa have long cultural sequences that include ESA, MSA and LSA industries, so Olieboomspoort, like Cave of Hearths, is truly exceptional. Equid teeth from the MSA at Olieboomspoort were dated by U-series-ESR estimates to 150±14 ka ago (Val et al. 2021). Bushman Rock Shelter has a deep MSA sequence overlain by LSA. Its hornfels-dominated MSA assemblages (Plug 1981; Porraz et al. 2015) now have ages that place some of the uppermost MSA occupations at about 100 ka ago (Porraz et al. 2018).

Open-air MSA sites excavated below the Waterberg escarpment include Blaaubank, Kalkbank and Wonderkrater. Blaaubank, in a gravel donga near Rooiberg, has a wealth of MSA tools overlying ESA ones (Mason 1962), while Kalkbank, also with some MSA lithics (Mason 1962), generated many broken animal bones that are now known to have been accumulated predominantly by non-human agents (Hutson & Cain 2008). Wonderkrater, which is near Mookgophong (formerly Naboomspruit), is an MSA spring and peat site. It has ages (derived from optically stimulated luminescence (OSL) dating of quartz grains) of between about 100 and 30 ka ago (Barré et al. 2012; Backwell et al. 2014). Unfortunately, there are few stone implements around the spring and they cannot be securely attributed to anything other than a generic MSA industry. Most seem to be cutting tools made on rhyolite (Backwell et al. 2014).

The higher altitude Waterberg plateau has received much less archaeological attention than the surrounding regions. A small rock shelter, North Brabant (New Belgium 608 LR), was excavated in the 1960s by Schoonraad and Beaumont (1968), and here the MSA component of the site was attributed to a 'Middle Pietersburg' industry. Van der Ryst (1998) re-excavated this shelter and recovered MSA unifacial points at its base. Van der Ryst's (1998) excavations in other plateau sites revealed that LSA occupation in the Waterberg was essentially contemporaneous with that by

Iron Age farmers; hunter-gatherers seem to have followed farmers onto the plateau, where a symbiotic relationship existed until populations became untenably large for this rather marginal environment. Interestingly, although the Waterberg sites that Van der Ryst excavated yielded LSA occupations dating only to the last 1 000 years, several of them had MSA occupations immediately under the LSA ones, implying a long occupation hiatus of unknown age, but minimally of about 25 ka because the final MSA dates to about this time. There are extensive remains of MSA occupations on the Waterberg plateau, mostly in the form of stone tools scattered near water sources, but until the work at Red Balloon Rock Shelter, none of these MSA sites had been dated. LSA artefacts radiocarbon dated to the 10th and 12th centuries AD were recovered from several younger occupations (Van der Ryst 1998). A few MSA blades and a broken point were later found in a rock shelter at Schurfpoort 112KR on the Waterberg plateau (Van der Ryst 1998). At Goergap 113KR rock shelter, also on the plateau, Van der Ryst (1998) excavated a substantial MSA stone tool collection. At the base, the tools were generally longer than 50 mm and the length of some quartzite blades exceeded 150 mm. Points and knife-like tools were also common. In the younger MSA layers of Goergap 113KR, the tools were smaller and there was a change in rock type from quartzite to felsite. Such technological change implies that this site was settled on multiple occasions, though probably not continuously, during the MSA.

The Steenbokfontein 9KR spring open MSA site on the plateau is surrounded by outcrops of fine-grained siltstones that are exposed around the eyes of springs and in local river cuttings (Wadley et al. 2016). The rocks belong to the locally restricted Vaalwater Formation, the youngest part of the Waterberg succession (Jansen 1982). The Vaalwater beds were probably deposited in the shallow water of a small inland lake (Jansen 1982: 53) about 40 km wide, between Vaalwater and Dorset (De Vries 1970, 1973). Subsequently, the siltstone was hardened when diabase intrusions caused contact metamorphism (De Bruiyn 1971: 6). Some siltstones were silicified (De Vries 1970; Jansen 1982: 50), making them suitable for tool making, so the area is littered with knapping debris. This siltstone was transported to other Waterberg Stone Age sites, including Red Balloon Rock Shelter, to be discussed shortly. At Steenbokfontein 9KR the spring was repeatedly visited by humans and animals, and the lithics are trampled (De la Peña & Witelson 2018).

After the MSA occupations, the plateau seems to have been deserted until the arrival of Iron Age agropastoralists.

Background to Iron Age settlement

Based on unpublished data collected before his untimely death, Jan Aukema differentiated three phases of Iron Age settlement below and on the Waterberg plateau, and suggested that additional phases might also exist there (Huffman 1990). Aukema's survey in the 1980s of the Motlhabatsi River drainage basin, a tributary of the Limpopo River, revealed evidence for initial Iron Age activity on the farm Diamant, in the sweetveld at the foothills of the western Waterberg. Decorated ceramics of the Happy Rest facies, made by the first agropastoralists to occupy Diamant, were associated with a date of 1380±50 BP (Pta-3616) (Huffman 1990). A second occupation, which was dated to 1240±50 BP (Pta-3620), is associated with

Zhizo series glass beads and is linked to the Diamant facies, the successor to the Happy Rest facies. These early agropastoralists brought Middle Eastern glass beads to the Waterberg (Wood 2005) (perhaps obtained from Schroda on the Limpopo, which would have been on the international ivory trade route), as well as decorated pottery, cattle, sheep and indigenous crops like sorghum and millet, although they still consumed game meat and wild plant foods. Iron working also took place at Diamant (Huffman 2007), and smelting sites are fairly common in the Waterberg and its foothills. Today iron is commercially mined at Thabazimbi, which is in close proximity to Diamant and where a rich iron ore body was probably also accessed by people from the Waterberg Iron Age villages.

Aukema's second phase, represented by the Eiland facies, began in the 11th century AD. One Eiland site, Wentzel, is near the Limpopo and Motlhabatsi confluence, where soil is rich and deep and therefore ideally suited to agriculture. Most recorded Eiland ceramics are, however, found in the sourveld of high river valleys on the Waterberg plateau. The high plateau seems to have been populated by many people by the 11th century AD, when farmers migrated there from the sweetveld of the lowlands. Perhaps the sweetveld had been overgrazed, encouraging tsetse fly infestation (Huffman 1990); the plateau, however, is too high for these dangerous pests. The immigrants made the distinctive Eiland ceramics with herring-bone motifs that were used between the 11th and 14th centuries. Such ceramics were recovered from the farm Kirstenbos 497LR, near Marken, where both LSA and terraced Middle Iron Age settlements were found (Van der Ryst 1998). Unlike this site, the hilltop village of Ongelukskraal 48KR has both stone-walling and Eiland ceramics (Van der Ryst 1998). Ongelukskraal 48KR is below the vertical cliffs of Tafelkop, and was excavated by Aukema in 1989 and Boeyens in 1991. In the centre of the stone-walled complex are steep cliffs and shelters with fine-line rock paintings. A single date of 1850±50 BP (Pta-5161, calibrated to AD 144 (233) 258) was obtained for a layer containing two Bambata potsherds, grindstones and a few quartz flakes (Van der Ryst 1998: 24). Excavations at the Olieboomspoort uncovered the richest collection of Bambata ceramics in the Waterberg area (Van der Ryst 2006). The presence of Bambata ceramics at Olieboomspoort and Ongelukskraal 48KR implies pre-Early Iron Age occupation on the plateau, either by LSA communities who made or obtained the ceramics through trade, or possibly by herders or agropastoralists who had contact with settlements like Toteng in Botswana, where Bambata ceramics are abundant (Huffman 2007). Huffman (2007) favours an interpretation of hunter-gatherers obtaining the pottery through trade.

A substantial collection of Happy Rest facies (AD 550–750) as well as Eiland facies ceramics were recovered at Olieboomspoort. Ceramics of a fourth facies with decoration motifs similar to those of the Icon facies (early Moloko, AD 1350–1500) were also identified. Some of these 'Icon' bowls were still covered with red ochre paint residues, demonstrating that they were used for holding paint. It can be argued that some of the rock paintings in the shelter were done by using these vessels as containers for the paint, though they may have been linked to other ritual activities there. Eiland ceramics and grindstones are frequently found in crevices or small rock shelters on the hilltops or cliffs of the Waterberg. These rock shelters are generally unsuitable for habitation, even for defence, and it is likely that the pots and grindstones were

amongst the offerings made at rain-making ceremonies (Aukema 1989). At these rituals an appeal for rain was made to the ancestors (Aukema 1989). The grindstones were for grinding medicines such as herbs that were then mixed and stored in pots. Many of the paintings in the small shelters are also likely to have been linked to rain-making.

Aukema's third phase is the Later Iron Age, associated with stone-walled villages and undecorated pottery on hilltops. These settlements may coincide with the 16th and 17th century AD arrival of Nguni speakers (probably Northern Ndebele people). Aukema excavated the defensive hilltop site Buffelsfontein (Kb8) in the western Waterberg, dated 330±50 BP (Pta-3612) (Huffman 1990, 2007). He uncovered remains of beehive-shaped huts on small terraces behind kraals, and these were most likely produced by an Nguni-speaking group (Huffman 2007: 448). Buffelsfontein's undecorated globular pots are not like Moloko ware, and support other evidence (Huffman 2007: 448) that this was not a Sotho-Tswana settlement. Similar stone-walled sites were also recorded in the vicinity of Red Balloon Rock Shelter, and there is a prominent settlement on top of Marong Hill.

In the 17th century AD, the ancestors of the Northern Sotho and Tswana peoples settled in the sweetveld near the Motlhabatsi River, as earlier Iron Age farmers had done (Huffman 1990). These farmers created multi-chrome Moloko pottery with dragged punctate bands, and bands burnished with red ochre and black graphite associated with the Letsibogo facies. At the same time, other Sotho-Tswana communities settled around the foothills of Thabazimbi and Rooiberg (Hall 1981), and these settlements can be linked to the Madikwe and Rooiberg facies respectively (Huffman 2006, 2007). Some Moloko pottery was found at Kirstenbos, and might have been associated with rain control since the site was a prominent Eiland rain-control hilltop site (Van der Ryst 1998). Nevertheless, Moloko pottery was absent from both Buffelsfontein and Melora Hilltop. By the 18th century there were large Later Iron Age communities in the area, competing with each other and hunter-gatherer (San) groups for scarce resources. The resulting tensions caused the San to flee north or west, though some stayed because of intermarriage with farmers.

To the east of the Waterberg, the Pedi (a group of Northern Sotho) became powerful in the 18th century, perhaps because of their control over trade networks (Delius 1983). In 1822 the situation changed when the Ndebele, led by Mzilikazi, defeated the Pedi, at the same time triggering food shortages in the area. The devastation to Northern Sotho and Tswana areas continued for fifteen years until a Tswana and Boer army evicted the Ndebele, who fled to Zimbabwe. This was a period of considerable raiding and many people hid in the mountains. Small groups took refuge in rock shelters and caves, while others hid their villages in remote parts of the mountains. One such 19th-century refuge site is in the saddle of Melora Hilltop. It yielded Moloko pottery, probably made by Sotho-Tswana. Soil erosion exposed stone-built granary platforms, hut rubble that included daga (burnt clay) flooring, ceramics, lower and upper grindstones, copper bangles, a copper earring, iron slag and tools, glass beads, a clay spindle whorl and a rhinoceros clay figurine (Boeyens et al. 2009; Boeyens & Van der Ryst 2014). The radiocarbon date of 120±45 BP (Pta-5139) supports oral tradition about the area as a refugium during the *difaqane*. This is probably the context within which a small group of agropastoralists sought refuge in Red Balloon Rock Shelter, as we explain shortly.

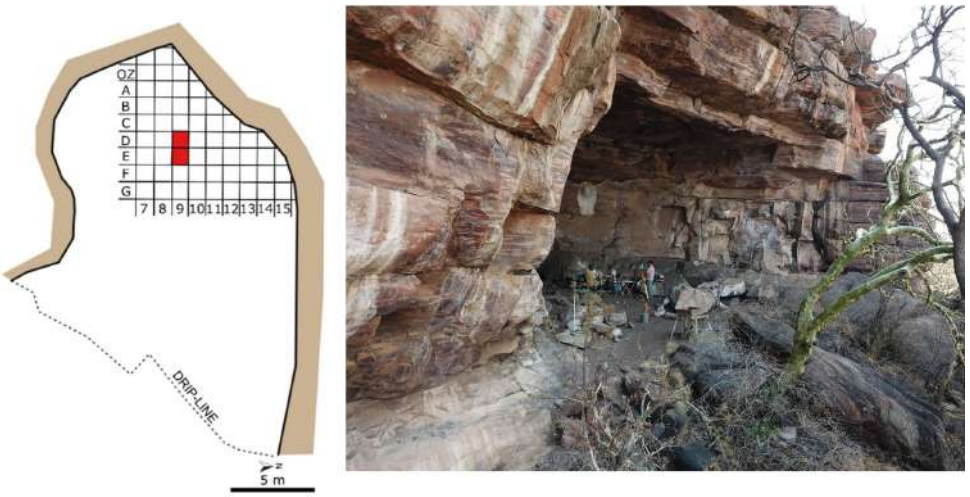

Fig. 2. Red Balloon Rock Shelter mapped with the total station (left). Squares D9 and E9 were partially excavated. Right: the shelter entrance.

RED BALLOON: DESCRIPTION OF THE ROCK SHELTER AND ITS SURROUNDS

Red Balloon Rock Shelter (Fig. 2) is on the north-western edge of the Waterberg plateau, about 30 km south of Lephalale and about 15 km from Olieboomspoort that lies below the escarpment (Fig. 1). The shelter is at an altitude of about 1 200 m above mean sea level on an east-facing sandstone cliff that is strung with small rock shelters like beads on a necklace. In the valley is a stream bed that fills with water after rain. The region is warmer than the southern and eastern parts of the Waterberg plateau, and the mean rainfall of the area is approximately 600 mm per annum (mostly summer rainfall). The vegetation is predominantly broad-leaved savanna and *Acacia* veld. Various trees and shrubs growing on the hillside near Red Balloon Rock Shelter and in the valley below the shelter were recorded (Table 1). The list is not comprehensive because during the survey most trees and shrubs were leafless and started to bud only after the first spring rains, which fell during the late September excavation of the shelter. The cliff face supports, among other trees and shrubs (Table 1), *Commiphora marlothii* (papierbaskanniedood), *Sterculia rogersii* (star chestnut), a variety of small shrubs like *Grewia* spp. and *Obetia tenax*, and the showy *Erythrophysa transvaalensis* (bushveld red balloon tree), with its distinctive seedpods for which the shelter is named.

The shelter entrance is asymmetrical (Fig. 2), but has a dry living area of greater than 20×12 m. No plants grow inward of the dripline, and modern conditions in the shelter seem to preclude the entry of water. Small caverns against the back wall in the southern part of the shelter lead to deep tunnels that are still regularly used as dens by leopard and brown hyena. The desiccated remains of a waterbuck carcass lie in one tunnel. The shelter attracted our attention because the surface is strewn with MSA lithics and Iron Age ceramics. Furthermore, organic preservation seemed likely because of the dry floor on which no vegetation grows. Red Balloon lacks rock art, but an adjacent shelter has a few red fine-line paintings and white finger paintings, two of which appear to be spread hides (Laue 2001).

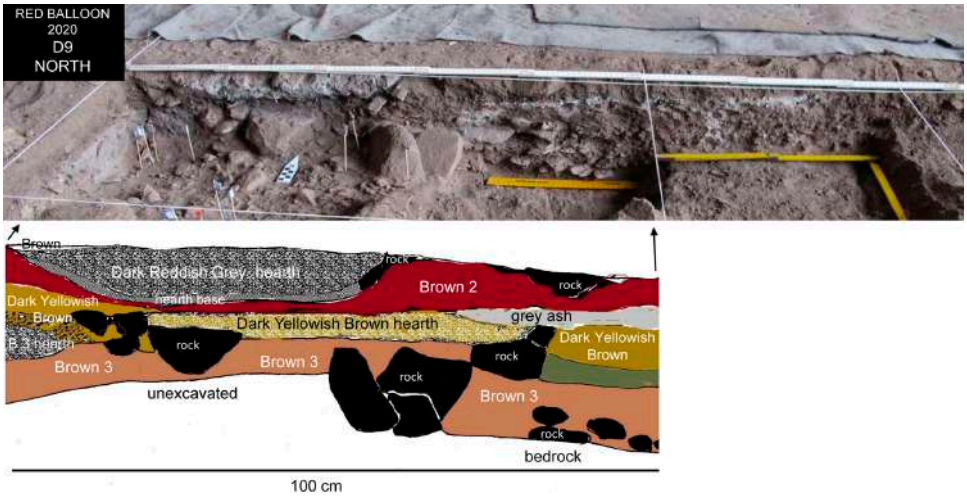

Fig. 3. Red Balloon north wall stratigraphy of square D9, with one quadrant of square E9 to the right. The yellow ruler is on bedrock. The upper ash units visible below the white tape are Iron Age hearths, but layer Brown 3 below the name sign is Middle Stone Age (labelled B3 Hearth).

METHOD

A 2×1 m grid (consisting of metre squares named D9 and E9) was aligned north (Figs 2 and 3) and the excavation was conducted in September 2020. A permanent datum point comprising a metal stake set in concrete was placed at the north-east entrance. The site and all excavated finds larger than 2 cm were mapped with a Nikon Nivo 5C total station. Each layer and sub-layer surface (*décapage*) was photographed with both a Canon camera and a Microsoft Surface tablet. A *décapage* is the smallest coherent unit marked by the base of material lying on an archaeological surface (Val et al. 2021). The tablet images were imported into Endnote and all plotted artefacts were then assigned their total station number on the Endnote image using a Surface scribe. Standard excavation techniques were used and all excavated sediment was screened through 2 mm and 1 mm mesh. At the end of the excavation, the site was rehabilitated with a carpet of geotextile on the excavated surface, custom-made hessian sandbags filled with screened sediment, and a topping of raked, screened sediment.

A charcoal sample for ^{14}C dating was collected directly into an aluminium foil cone from an Iron Age hearth. The sample was processed by iThemba Labs at Wits University.

Fourier Transform Infrared Spectroscopy (FTIR) was conducted in a field laboratory on sediment crusts covering the lithics and Iron Age ceramics. FTIR analyses were carried out with a portable Bruker Alpha instrument equipped with an Attenuated Total Reflectance (ATR) module. Close contact was made between each crushed and homogenised sample and the ATR diamond crystal. The spectral resolution used was 4 cm^{-1} and the spectra were acquired with 64 scans between the wavelengths of 400 and 4000 cm^{-1}.

Sediment cores for optical dating were taken by hammering three 15 cm long plastic pipes, sealed at their base, into the section walls. The pipe openings were also sealed after removal; the samples were plotted with the total station and then sent to the University

of Wollongong's School of Earth, Atmospheric and Life Sciences with Australian Government permit 0004378957. Since archaeologists sometimes criticise dating methodology, we provide this in detail. Potassium (K)-rich feldspar grains (180–212 μm diameter) were isolated for optical dating, purified using standard procedures (e.g. Wintle 1997), and measured on automated Risø TL-DA-20 readers (Bøtter-Jensen et al. 2003). Infrared (IR) stimulation of individual K-feldspar grains was achieved using a focused laser beam (830 nm) (Bøtter-Jensen et al. 2003). Individual K-feldspar grains were mounted onto standard Risø single-grain discs (drilled with 100 holes that are each 300 μm in diameter and 300 μm deep) (Bøtter-Jensen et al. 2000), where each grain hole contained one grain. The infrared stimulated luminescence (IRSL) emissions were detected using an Electron Tubes Ltd 9235B photomultiplier tube fitted with Schott BG-39 and Corning 7-59 filters to transmit wavelengths of 320–480 nm. Irradiations were carried out using $^{90}Sr/^{90}Y$ beta sources, calibrated for individual grain positions using irradiated quartz standards of known gamma doses. Solar bleaching tests were conducted using a Dr Hönle solar simulator (model: UVACUBE 400).

For equivalent dose (D_e) determination, we applied a single-aliquot regenerative-dose (SAR) post-infrared infrared (pIRIR) procedure for individual K-feldspar grains (Thomsen et al. 2008), in which the single-grain pIRIR signal was measured at 275°C for 2 s using an IR laser after a prior-IR stimulation at a high stimulation temperature (200°C) for 200 s (Li & Li 2012). The details of the procedure are shown in Table 2.

Representative single-grain pIRIR decay curves from sample 3096 are shown in Figure 4a. Most of the grains have pIRIR signals that decay to a constant background level within the first 0.5 s of stimulation time. The net initial IRSL intensities of the test-dose signal (T_n), calculated by subtracting the signal of the first 0.1 s from that of the last 0.3 s, range from a few tens of counts per 0.1 s to a few tens of thousand counts per 0.1 s, but they are predominantly less than 3000 counts per 0.1 s (Fig. 4b). The cumulative light sum plot (Fig. 4c) shows that ~10% of the grains emitted more than 80% of total light.

To estimate D_e, we adopted a combined standardised growth curve (SGC) and L_nT_n method (Li et al. 2015b; Li et al. 2017; Li et al. 2020). To establish an SGC, a total of 800 grains from sample 3096 were measured with a full SAR pIRIR procedure. A series of regenerative doses (up to ~1500 Gy), including a zero dose and a repeat dose point, were measured to establish dose-response curves (DRCs) for individual grains. Several rejection criteria were used to reject grains with unsuitable behaviours or poor DRCs: 1) the initial test dose signal (T_n) is less than 3σ above the corresponding background count, or the relative standard error on T_n is >25%; 2) the ratio of the zero-dose sensitivity-corrected dose value (L_x/T_x) to the maximum regenerative-dose L_x/T_x value is >5%; 3) the L_x/T_x data points are too scattered, i.e., they have large figure-of-merit (FOM) and reduced chi-square (RCS) values higher than 10 and 5%, respectively (see Jacobs et al. 2019). This resulted in a total of 47 grains accepted for SGC establishment. We adopted the least-square normalisation (LS-normalisation) procedure (Li et al. 2016) to normalise the L_x/T_x data and used a general-order kinetics (GOK) function (Guralnik et al. 2015), in the form f(x) = a*[1−(1+b*c*x)(−1/c)]+d, to fit the normalised data. The LS-normalised L_x/T_x data and the corresponding SGC are shown in Figure 4e. The figure indicates that different grains share the same dose-response pattern that can be well described by the SGC. To further validate the SGC, we have calculated and

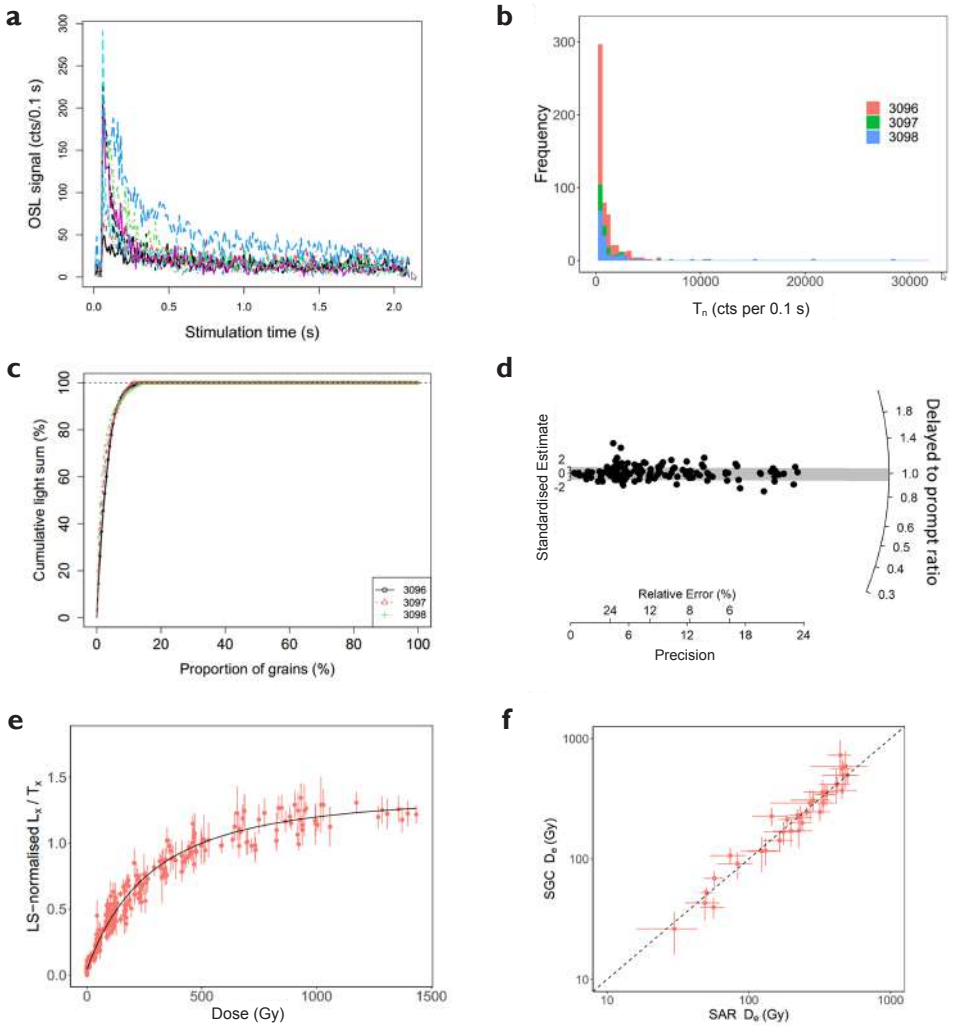

Fig. 4. (a) Representative post-infrared infrared (pIRIR) decay curves from 10 grains of sample 3096. (b) Histogram of the distribution of Tn intensity of pIRIR signals from individual K-feldspar grains of different samples. (c) Cumulative light sum of single-grain K-feldspar pIRIR for different samples. (d) Delayed-to-prompt signal ratios ('fading ratio test') for individual grains from sample 3096. (e) Least-square-normalised Lx/Tx data and best-fit standardised growth curve (SGC). (f) Comparison between SAR D_e (single-aliquot regenerative-dose equivalent dose) and SGC D_e values. The broken line represents the 1:1 ratio.

compared the D_e values based on the SGC and their corresponding individual DRCs, using the procedure proposed by Li et al. (2015a). The SGC D_e values are plotted against their corresponding SAR D_e values in Figure 4f, which shows that the SGC and SAR D_e values are indistinguishable from each other, and confirms that the SGC is reliable. We therefore applied the SGC procedure to the other two samples and some additional grains from 3096, by only measuring the signals from the natural dose (P) and an additional regenerative dose (D_r) and their corresponding test doses. D_r is a

regenerative dose similar to the size of the expected P, and its signal (L_r/T_r) was used for normalising the natural signal (L_n/T_n). To determine the final D_e value for each sample, we adopted the L_nT_n method (Li et al. 2017) by analysing the distribution of the SGC-normalised L_n/T_n signals using different statistical models and then projecting the final L_n/T_n estimate onto the established SGC to obtain a final D_e.

The suitability of the pIRIR and SGC procedure was tested using dose recovery, residual dose and anomalous fading tests. For the dose recovery and residual dose tests, a total of 700 grains of sample 3096 were bleached using the solar simulator for >8 hours. Four discs of the bleached grains (n = 400) were given a laboratory dose of ~200 Gy, and they were measured using the pIRIR SGC procedure described above. A D_e value of 194±8 Gy was obtained, corresponding to a recovery ratio of 0.97±0.04. This suggests that the known dose can be successfully recovered using the SGC and L_nT_n methods. For the residual dose test, 300 bleached grains were measured directly with the pIRIR procedure, which resulted in a residual dose of 2.7±2.2 Gy, which is negligible and, hence, we do not make any correction for residual dose.

To test whether the pIRIR signal suffered from anomalous fading, after the measurement of dose recovery and residual dose, the measured grains were given a regenerative dose of ~200 Gy. They were then preheated and stored in the dark at room temperature for several days, corresponding to a time delay of 2.3 decades compared to the prompt measurement. The pIRIR signals after delay were then measured. After that, the same regenerative cycle was repeated but without any delay between preheat and pIRIR measurements. We then calculated the ratio between the pIRIR signals measured after delay and those without delay (the so-called 'delayed to prompt ratio'). The delayed to prompt ratios for a total of 144 luminescent grains are shown in Figure 4d. Most of them are consistent with unity at 2σ, and the weighted mean of the ratios is 1.00±0.01, suggesting that the pIRIR signal for our samples had negligible fading. We therefore did not make any fading correction for our calculated ages.

Environmental dose rates were calculated as the sum of the beta, gamma and cosmic-ray dose rates external to the grains, plus an internal beta dose rate due to the decay of potassium within the K-feldspar grains. We assumed that present-day radionuclide activities and dose rates have prevailed throughout the period of sample burial. Beta and gamma dose rates were estimated from uranium, thorium and potassium concentrations obtained from a combination of inductively coupled plasma mass spectrometry (ICP-MS) and optical emission spectroscopy (ICP-OES), and converted to dose rates using the conversion factors of Guérin et al. (2011). Beta dose rates were corrected for grain size (Brennan 2003). Cosmic-ray dose rates were calculated following Prescott and Hutton (1994), adjusting for site altitude, geomagnetic latitude, and the density of sediment and rock, and thickness of sediment and rock overburden. Beta, gamma and cosmic-ray dose rates were corrected for a moisture content of 5±2% for all three samples (Nathan & Mauz 2008). The D_e divided by the environmental dose rate gives the burial time of the grains in calendar years.

The larger macrobotanical remains, such as the stones (endocarps) of marula (*Sclerocarya birrea*), and buffalo-thorn (*Ziziphus mucronata*), were plotted with the total station and removed individually during excavation. All macrobotanical remains visible to the naked eye were collected from the 2 mm sievings, and these and individually plotted material were stored in small ziplock packets placed in hard plastic bottles. Seeds

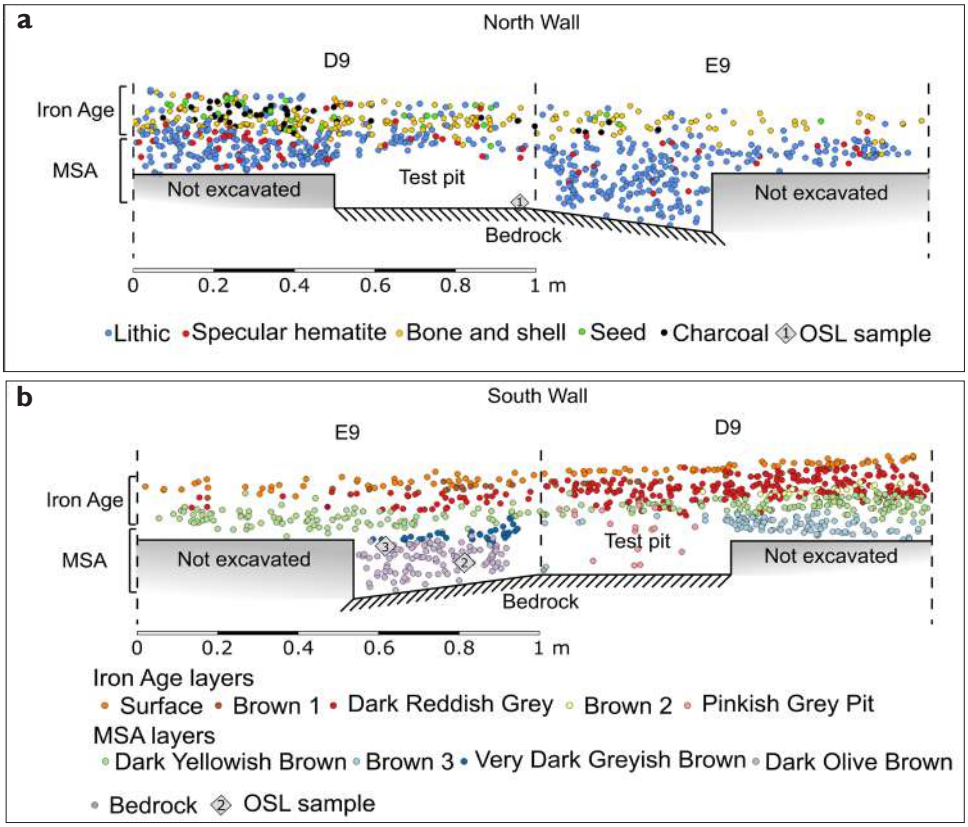

Fig. 5. Red Balloon Rock Shelter total station plots in squares D9 and E9. (a) North wall projection of all finds and OSL sample 1. (b) South wall showing the layers and the position of OSL samples 2 and 3. Plotting was not regularly done in the test pit 50 cm quadrant because of time constraints. Layers are not continuous across both squares or sometimes even across one quadrant.

were not collected from the 1 mm sievings because mixing of the sediments in which they were preserved indicated that the dubious rewards of such a time-consuming task were not justified. Taxa removed in situ and from the 2 mm sievings were identified but not quantified in any detail for the same reason.

RESULTS

Notwithstanding the large size of the rock shelter, the sediment is shallow (Fig. 3). The upper strata with Iron Age material preserved organic remains (Fig. 5), but there is no organic preservation in the older MSA layers, although stratigraphy can be recognised. Two ashy hearths are preserved in the MSA, but preservation is so poor that few charcoal fragments were recovered.

The Middle Stone Age occupations

The basal layers with MSA lithics are rocky, except for the two ashy areas that were probably hearths, and the lithics on bedrock are coated with dried mud and a thin film

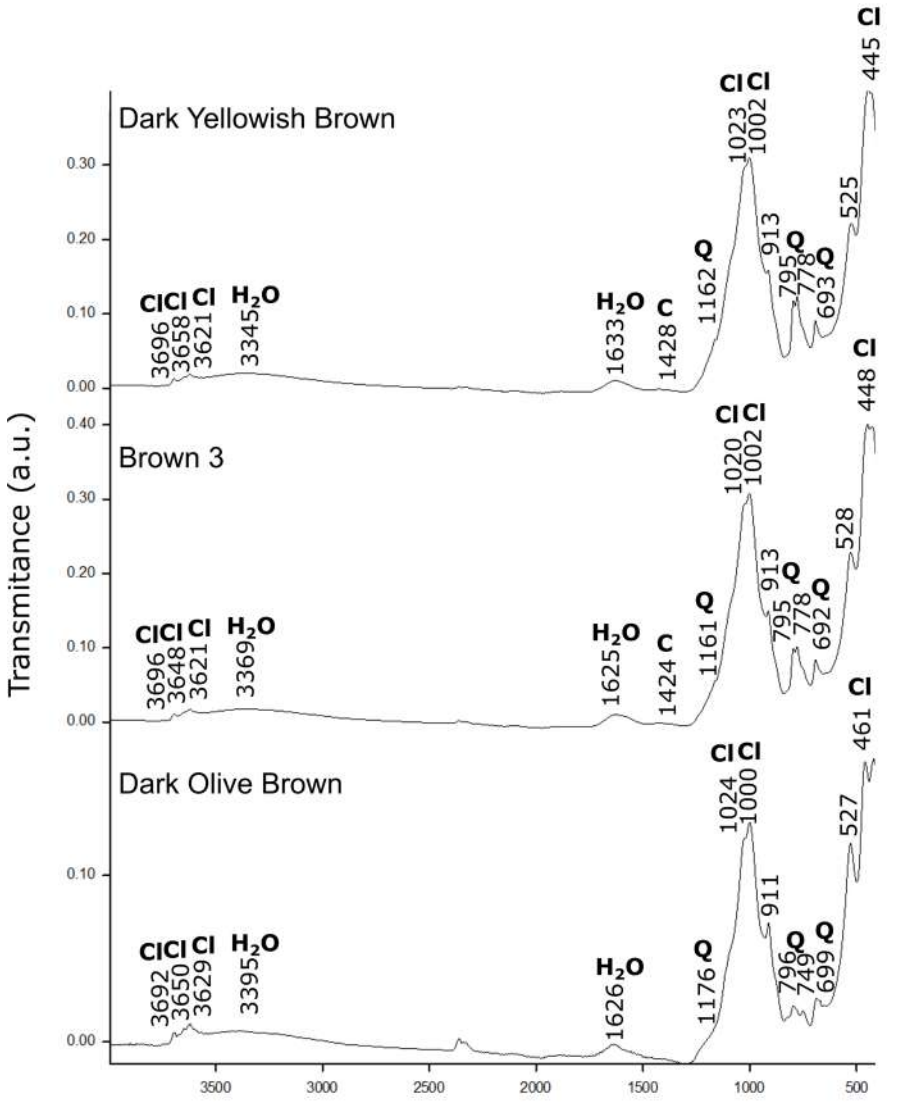

Fig. 6. Red Balloon Rock Shelter FTIR spectra of the analysed sediment crusts covering the lithics. C = calcite; Cl = kaolinite clay; Q = quartz.

of calcite. Dried mud is thickest on the lithic under-surfaces. We made fine distinctions between strata and features, and the layers are listed in Table 3.

FTIR analyses performed on sediment crusts covering the lithics from undisturbed MSA layers (Dark Yellowish Brown, Brown 3, Dark Olive Brown) aimed at getting a better understanding of the taphonomy of the site. Spectra collected on these crusts are similar (Fig. 6). Bands at 445 (Si-O bending), 1002 (Si-O stretching), 1023 (Si-O stretching), 3621, 3658 and 3696 cm^{-1} dominate all three spectra and are interpreted as bands representing clay of the kaolin family (Müller et al. 2014). Another major component of these crusts is quartz, which was detected by the vibrational bands

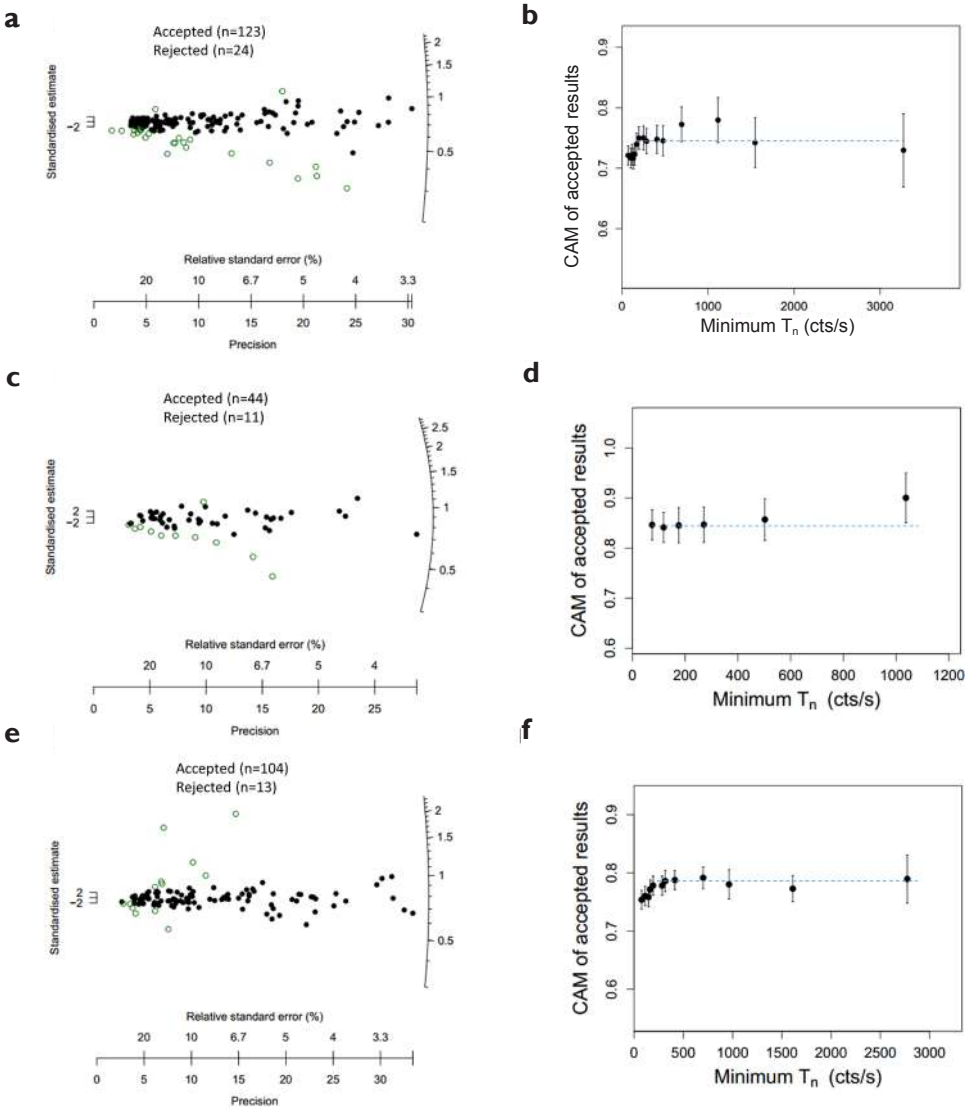

Fig. 7. Radial plots to the left show distributions of re-normalised L_n/T_n ratios for K-feldspar grains for (a) 1-1023, (c) 2-1024, and (e) 3-1056. The open circles are outliers identified by normalised median absolute deviation (nMAD). Plots to the right show the nMAD CAM re-normalised L_n/T_n ratios plotted as a function of T_n threshold for each sample. The blue stippled lines represent the plateau region of the re-normalised L_n/T_n ratio.

at 693 (symmetric Si-O bending), 778–795 (doublet, symmetric Si-O stretching) and 1162 (shoulder, asymmetric Si-O stretching) cm^{-1}. Adsorbed water was detected from the weak feature around 1630 (O-H bending) and 3350 (O-H stretching) cm^{-1}. A weak feature around 1425 cm^{-1} (carbonate asymmetric stretch), characteristic of calcite (calcium carbonate), is present on the spectra of the crust found on the lithics from layers Dark Yellowish Brown and Brown 3. Fresh wood-ash is predominantly

calcite, which undergoes solubilisation/precipitation cycles in wet conditions. As numerous hearths were found in the upper part of the MSA sequence, calcite from those hearths must have solubilised, circulated, and mixed with clay of kaolin type during wet conditions.

Optically Stimulated Luminescence dating of sediments

We measured 1 700, 1 000 and 1 000 grains from samples 1-1026, 2-1027 and 3-1056, respectively. The numbers of grains measured, rejected and accepted are summarised in Table 4. The distributions of the SGC-normalised L_n/T_n values for the accepted grains from all the samples are shown in Figure 7a, c and e. It shows that each of the samples has a distribution of D_e values that are dominated by a single-dose population, but with a small proportion of outliers. We identified these outliers using the normalised median absolute deviation (nMAD) (Rousseeuw et al. 2006) and rejected any log L_n/T_n ratios that had an nMAD value >2. We also applied the 'T_n threshold' procedure to test whether there is any dependence of D_e on signal brightness (e.g. Reimann et al. 2012; Jacobs et al. 2019; Guo et al. 2020). The T_n threshold results for each of the samples are shown in Figure 7b, d and f. Final D_e values are based on only the grains in the plateau region (dashed lines in Fig. 7b, d and f). To determine the final D_e value for each sample, the weighted mean L_n/T_n value, after application of nMAD, was calculated using the central age model (CAM) of Galbraith et al. (1999) and projected onto the SGC. For analysis of the luminescence data, the R packages numOSL (Peng et al. 2013; Peng & Li 2017) and Luminescence (Kreutzer et al. 2012) were used for curve fitting, D_e and error estimation, age model analysis and graphical display.

The total dose rates are similar for the three samples. External dose rates are based on laboratory estimates of U, Th and K, and do not take into account inhomogeneity in the gamma radiation sphere (~30 cm around the sample position). Notably, our estimates of the gamma dose rate assume that the bedrock has the same dose rate as the measured sediment. This need not be true and should be tested with direct measurements of the gamma dose rate in the field using a gamma spectrometer. Regardless, even if the gamma dose rate is wrong by 50%, the ages will only change within their respective two sigma uncertainties.

The De, dose rate and age estimates are summarised in Table 5. Uncertainties on the age are given at 1σ (the standard error on the mean) and were estimated by combining, in quadrature, all known and estimated sources of random and systematic error. The three age estimates of 91±6 ka (1-1023), 104±9 ka (2-1024) and 96±5 ka (3-1056) are statistically consistent within 1σ of each other. We combined the three age estimates to obtain a weighted mean age estimate of 96±4 ka ago for the MSA at Red Balloon Rock Shelter, suggesting that occupation likely occurred sometime during the period 92–100 ka ago (68.4% confidence interval). The resolution of the age estimates cannot resolve the duration of MSA occupation at the site.

Middle Stone Age lithics

The assemblage described here does not include the lithics that were mixed into the Iron Age pits, but all lithics from MSA layers (and associated features) Dark Olive Brown, Very Dark Greyish Brown, Brown 3 and Dark Yellowish Brown are described here.

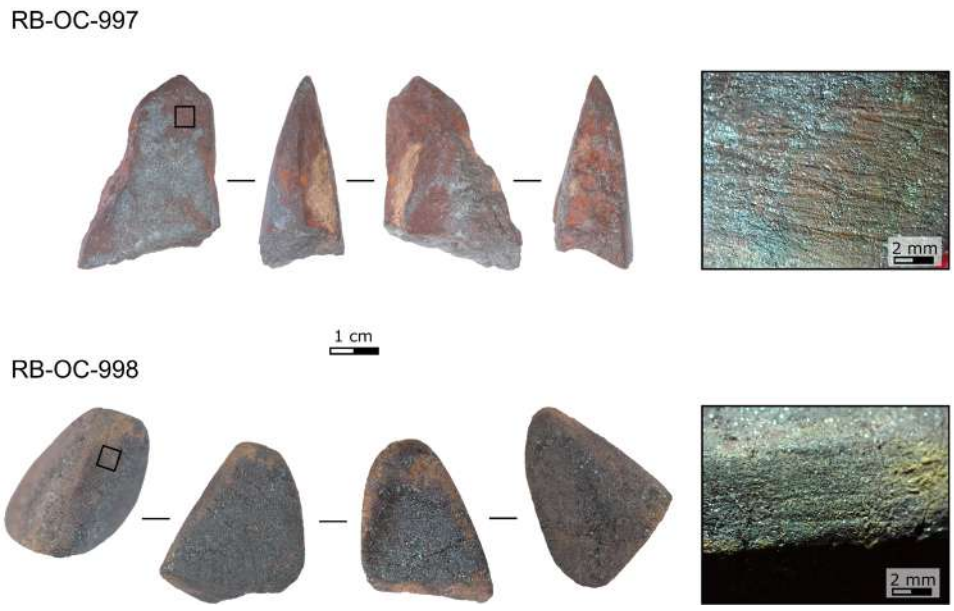

Fig. 8: Red Balloon Rock Shelter worked specular hematite recovered from Middle Stone Age layer Brown 3.

A wide variety of rocks and minerals was exploited for knapping: quartz, quartzite, jaspilite, fine- and coarse-grained sandstone, fine-grained siltstone, rhyolite and undifferentiated fine-grained basal igneous rocks (Table 6). Quartz nodules can be collected from the stream in the valley, and quartz and jaspilite pebbles also erode from the local conglomerate, which has a sandstone matrix. Fine-grained siltstones derive from the Vaalwater Formation. This is the origin of the siltstones used at Red Balloon Rock Shelter and they must have been transported for at least 30 km from their closest source. The lithics from the basal layers of the MSA occupation (Dark Olive Brown and Very Dark Greyish Brown) are heavily encrusted with dried clay, under which there is also a dull calcite patination. Noticeably, the clay crusts tend to be thickest on the underside of the lithics, that is, the face lying on the shelter floor. The crusts made it difficult (or impossible) to identify the rock types of the small pieces, so not all are listed in Table 6. Soaking in hot, soapy water did not remove the crusts adequately.

The presence of cores, core trimming flakes and many chips (Table 7) in the lithic assemblage shows that raw materials were often brought back to the shelter for knapping. Cortical flakes also demonstrate on-site knapping; smooth cortex is mostly present on quartz and quartzite flakes, suggesting that the source was river cobbles and possibly nodules that weathered from conglomerate. Although there are blades and blade fragments, the assemblage is geared more towards flake production, including that from prepared cores using the Levallois technique (Table 8). Whole flakes and blades have a fairly high volume density; 5.25 were found in each litre of sediment.

Nodules of specular hematite were also transported to the shelter; relatively few of them display grinding (Fig. 8) and a detailed analysis will be published separately. Only pieces found in the MSA context are discussed here; those from the Iron Age pit found with a mixture of MSA and Iron Age artefacts are excluded. The specular

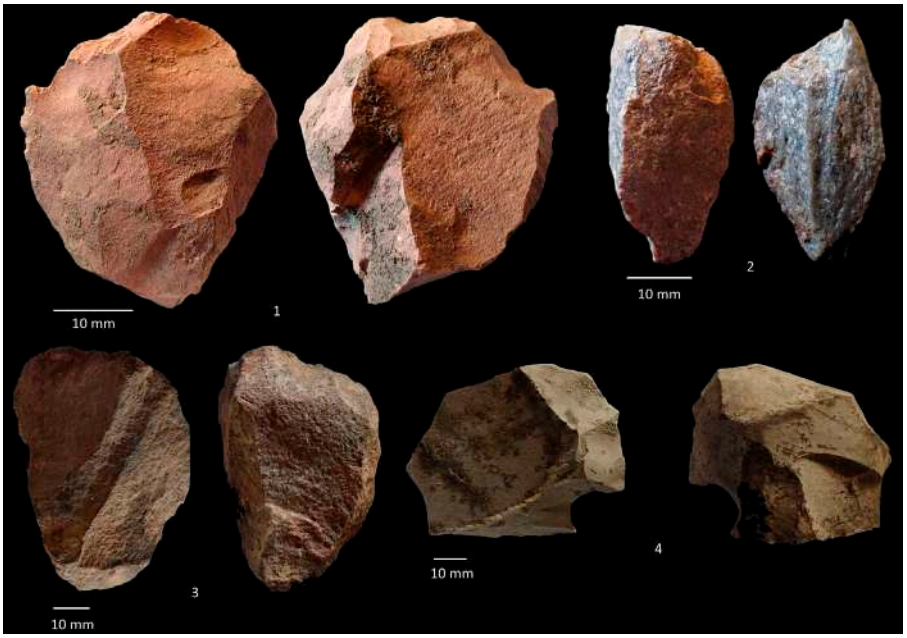

Fig. 9. Red Balloon Rock Shelter selection of Middle Stone Age cores. 1, 3, 4: Levallois cores; 2: casual core.

hematite pieces larger than 10 mm (Table 7) have a mass of 2 277.6 g and those smaller than 10 mm have a total mass of 196.8 g. We noted that these hematite nodules were most densely clustered on the perimeters of ash features that we interpret as hearths.

Apart from the prepared cores (for example, Levallois and radial/centripetal cores), there is a surprisingly large assemblage of small bipolar cores (Table 8, Figs 9 and 10) on quartz and quartzite. The flakes or bladelets from these cores were sometimes fashioned into tools like micro-notches. Levallois cores were most often preferential (designed for one removal of a predetermined shape), but some recurrent Levallois cores (producing more than one flake) were also found. The density of cores is relatively high, at about one core in every litre of deposit.

A wide range of retouched pieces was recovered (Table 9, Figs 11 and 12). Although broken tools represent the largest category, whole tools are dominated by side scrapers. Points are uncommon, most are unifacial, but a few poorly made bifacial points occur. Backed tools include a segment and a truncated blade (obliquely backed blade). Notches and denticulates are informally produced with irregularly spaced removals, some of which may be use-related. The chisel, adzes and notch imply the working of hard materials like wood or bone, but no organic preservation is present to test this hypothesis. Some noteworthy pieces include a micro-notch (Fig. 11: 2) that may have been a barb to be hafted on weaponry, and a small tanged point. The density of retouched pieces is 0.68 pieces per litre of sediment.

Iron Age use of the shelter

The excavation was too small to estimate with certainty the extent of Iron Age settlement in the shelter, but visits seem to have been ephemeral and occasional over

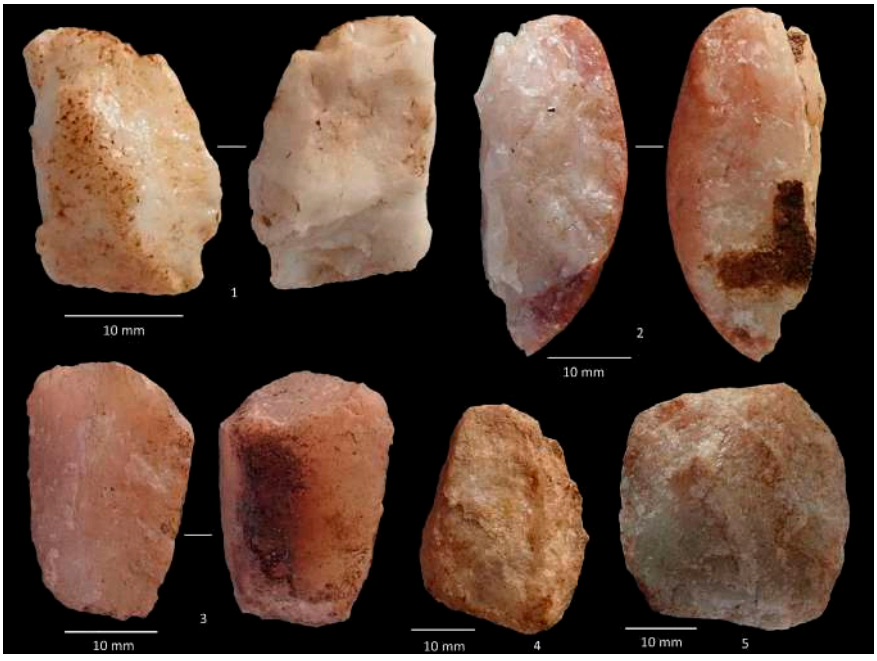

Fig. 10. Red Balloon Rock Shelter selection of Middle Stone Age bipolar cores.

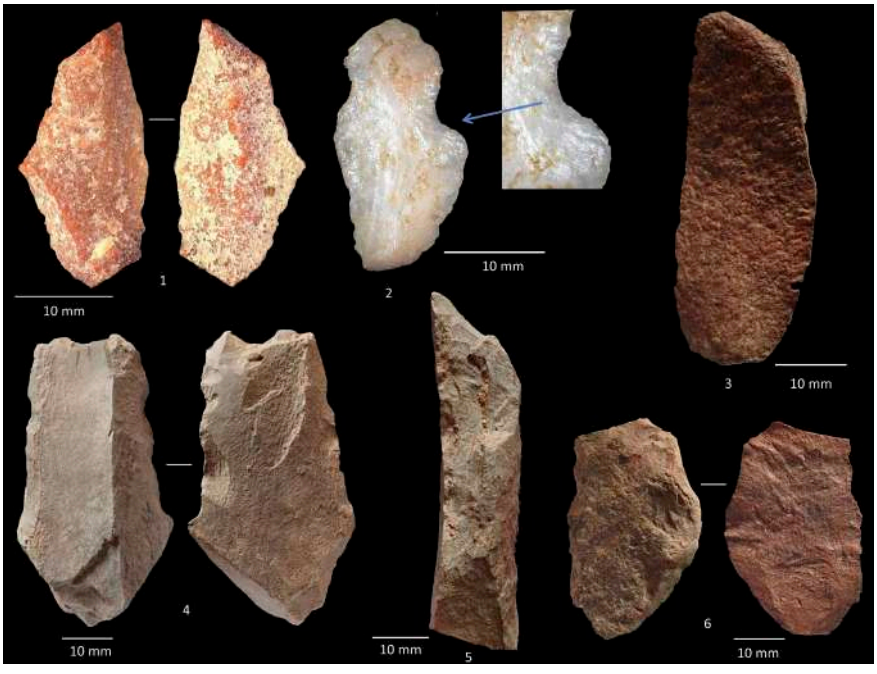

Fig. 11. Red Balloon Middle Stone Age formal tools. 1: backed tool on quartzite; 2: micro-notch on quartz, showing notch enlarged; 3: backed truncation on quartzite blade; 4: chisel on siltstone; 5: adze/awl on siltstone; 6: denticulate on rhyolite.

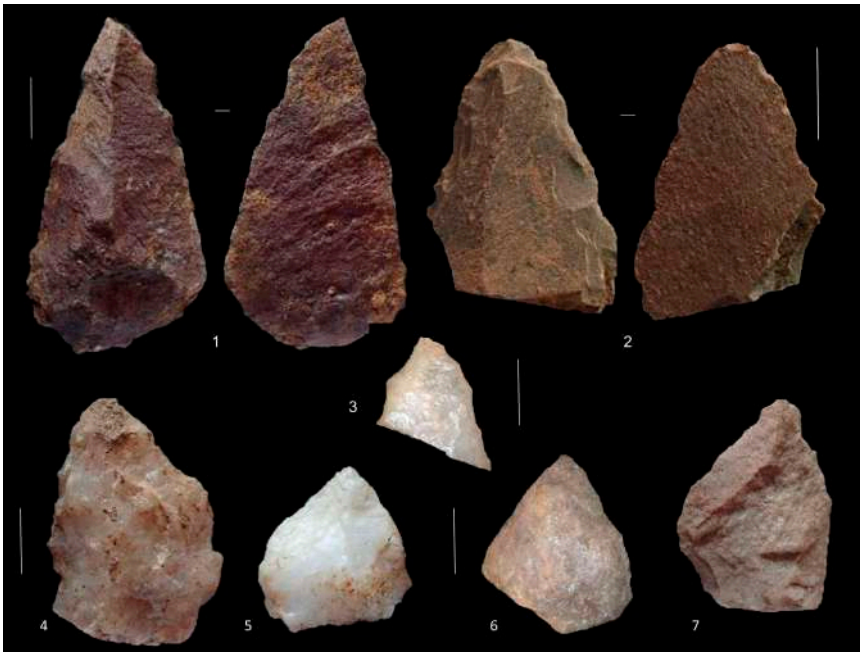

Fig. 12. Red Balloon Rock Shelter examples of Middle Stone Age unifacial, bifacial and Levallois points (unretouched, shaped point). 1: unifacial point, rhyolite; 2: broken unifacial point, siltstone; 3: bifacial point tip, quartz; 4: unifacial point, quartz; 5, 6: bifacial points, quartz; 7: Levallois point, quartzite. Each scale bar is 1 cm.

a relatively long period. People left behind Iron Age ceramics representative of several facies and most were recovered as surface finds. Nonetheless, our 2 m^2 trench revealed a large hearth with a pit dug into it (Fig. 13). This pit contained some undecorated ceramic sherds, smashed, unidentifiable burned bone from small bovids, and MSA lithics that had been displaced by the Iron Age activity. Organic preservation was good in these layers and we recovered seeds, bone, shell and charcoal. The radiocarbon date on charcoal from a hearth in layer Dark Reddish Grey (Plan 1) is 250±80 BP (iTh-C-3303) (d13C=-22.9). The standard deviation is large because of difficulties associated with the radiocarbon curve at this time. No metal items were recovered and only one glass bead. Ostrich eggshell and snail shell beads were found, as well as some pieces of worked bone. We first describe the seeds, then the items of material culture.

Red Balloon Rock Shelter seed identification

The archaeobotanical assemblage from Red Balloon Rock Shelter has 28 different plant taxa (Table 10) that were identified by their seeds or other fruiting parts, to family, genus or species level. Edible fruits such as *Grewia* (raisin bush), *Searsia* (karee), *Z. mucronata* (buffalo-thorn), *Commiphora* (corkbush) and *S. birrea* (marula) characterise the assemblage. The taxa are all likely to occur around the shelter and in the adjacent valleys (Van Wyk & Van Wyk 2013). No macrobotanical remains were recovered from the MSA sediments, so all the seeds belong to the Iron Age and more recent past. Analysis of the preserved assemblage does not include any evidence of vegetation different

Fig. 13. Red Balloon Rock Shelter Iron Age pit into the hearth in layer Pinkish Grey.

from the current vegetation. Of special interest is *E. transvaalensis*, the striking bushveld red balloon tree after which the site is named. The species' distribution extends from Limpopo and the North West provinces into Botswana and Zimbabwe, and it is listed as Least Concern on the Red Data List (Van Wyk et al. 2016). The characteristic red balloon-like fruits (capsules) from the previous season were still on the trees in mid-September, and they began to sprout blossoms during our 16-day excavation season. The seeds are round and have a smooth and shiny deep reddish-brown surface, described as purple or black in some descriptions (e.g. Palmer & Pitman 1972; Van Wyk & Van Wyk 2013; Van Wyk et al. 2016). Some seeds even have neat round holes, presumably made by an unknown insect. These holes may have inspired and facilitated the stringing of the seeds, which are used as beads (Palmer & Pitman 1972). *Erythrophysa alata*, the Namaqua red balloon, has oil-rich seeds (Voigt 2010) and although no mention of oil in *E. transvaalensis* seeds was found, it is possible that they also have edible oil. *Pappea capensis* belongs to the same family, and there are many uses for its oil (Hankey 2004).

The frequencies of specific taxa were not calculated because mixing of the sediments rendered of little value the interpretations of relative frequencies between the layers. However, general observations, for example in Dark Reddish Grey, were that the assemblage was overwhelmingly dominated by *Grewia* spp. stones, followed by approximately equivalent frequencies of stones belonging to *Z. mucronata* and *Searsia* species. Other taxa were less common. There was considerable variation in the size and sometimes (although less marked) in the shape of the *Z. mucronata* stones, which suggests that perhaps a revision of the genus would be in order. Amongst the *S. birrea* remains, too, there was considerable variation in size. These size variations are noted, but no interpretations are proposed. Some seeds were covered with a fine coating of grey sediment, resembling smooth mud. Desiccated remains dominated over charred remains except in Pinkish Grey, where charred remains, mostly fragments, were present.

The desiccated remains were often coated with what appeared to be faeces containing many insect fragments. A possible explanation is that the seeds were eaten by baboon or civets and thereby deposited in the shelter. Not all seeds had passed through the gut of an animal; two *Grewia* cf. *flavescens* fruits with articulatd lobes would not have remained articulated if the fruit had been eaten.

Ceramics

Pottery occurs only in the Iron Age occupations. While many decorated sherds from several ceramic facies were recovered from the surface of the shelter, the excavation yielded only undecorated sherds. The surface collection of decorated and undecorated diagnostic (rim) sherds yielded representatives of Happy Rest, Diamant, Eiland and Letsibogo ceramic facies (see Table 11 and Fig. 14). Because of the surface disturbance in the shelter, most vessels were fragmented.

The surface collection totalled 82 vessels, of which 61 were decorated and 21 undecorated. These vessels had three main profiles: jars, constricted jars and deep bowls. The excavation yielded 70 undecorated indeterminate sherds (many of which were tiny fragments), two rim sherds and one broken ceramic lug.

The Happy Rest vessels constituted three recurved jars, with one revealing a thickened rim. A single long-neck jar represents the Diamant facies. The Eiland facies vessels are represented by 11 jars, one constricted jar and one bowl. The bowl body sherd was burnished with red ochre on the outside and inside of the vessel. The Eiland decorations were finely and neatly executed.

Four vessels had panels of parallel grooves and triangle designs filled in with parallel lines. The decorations were crudely executed. One sherd is ochre stained, probably from spilling of the ochre-mixed contents. In the Olieboomspoort ceramic collection a fair number of these crudely decorated vessels, some with ochre stains, were retrieved (Van der Ryst 2006). Their decoration motifs resemble the Red Balloon Rock Shelter ones, but also display rim notching. Van Schalkwyk (2000) also identified similar 16th-century decorated vessels that were excavated at Millbank in the Makgabeng Mountains.

The bulk of the collected decorated sherds can be ascribed to Tswana pottery (Moloko branch). The Letsibogo facies is represented by 14 jars, 7 constricted jars and 23 deep bowls. The bowls were burnished with graphite on the inside.

Analyses carried out on three ceramic sherds collected on the surface of the deposit aimed at exploring possible manufacturing differences between two Eiland sherds (Fig. 14: 9, 44) and an undecorated sherd. FTIR analysis of the three sherds revealed the presence of compounds commonly found in ceramics (Fig. 15). All three spectra are dominated by sundry clays and quartz, with minor contributions of water and calcite. The characteristic IR vibrational bands of quartz are located at around 520 (shoulder, asymmetric Si-O bending), 694 (symmetric Si-O bending), 778–795 (doublet, symmetric Si-O stretching), 1078 (shoulder, asymmetric Si-O stretching), and 1164 (shoulder, asymmetric Si-O stretching) cm^{-1} (Shillito et al. 2009; Müller et al. 2014).

From the spectra collected, it seems that the clays used to manufacture the different ceramics were different. Spectra recorded on the Eiland 1 sherd exhibit strong bands at 451 and 1027 cm^{-1}, which we interpret as part of a clay signal, with a weaker feature of calcite (calcium carbonate) at 1436 (carbonate asymmetric stretch) cm^{-1}. The Eiland 2 pottery sherd spectrum presents strong bands at 445, 992 and 1022 cm^{-1}, interpreted as

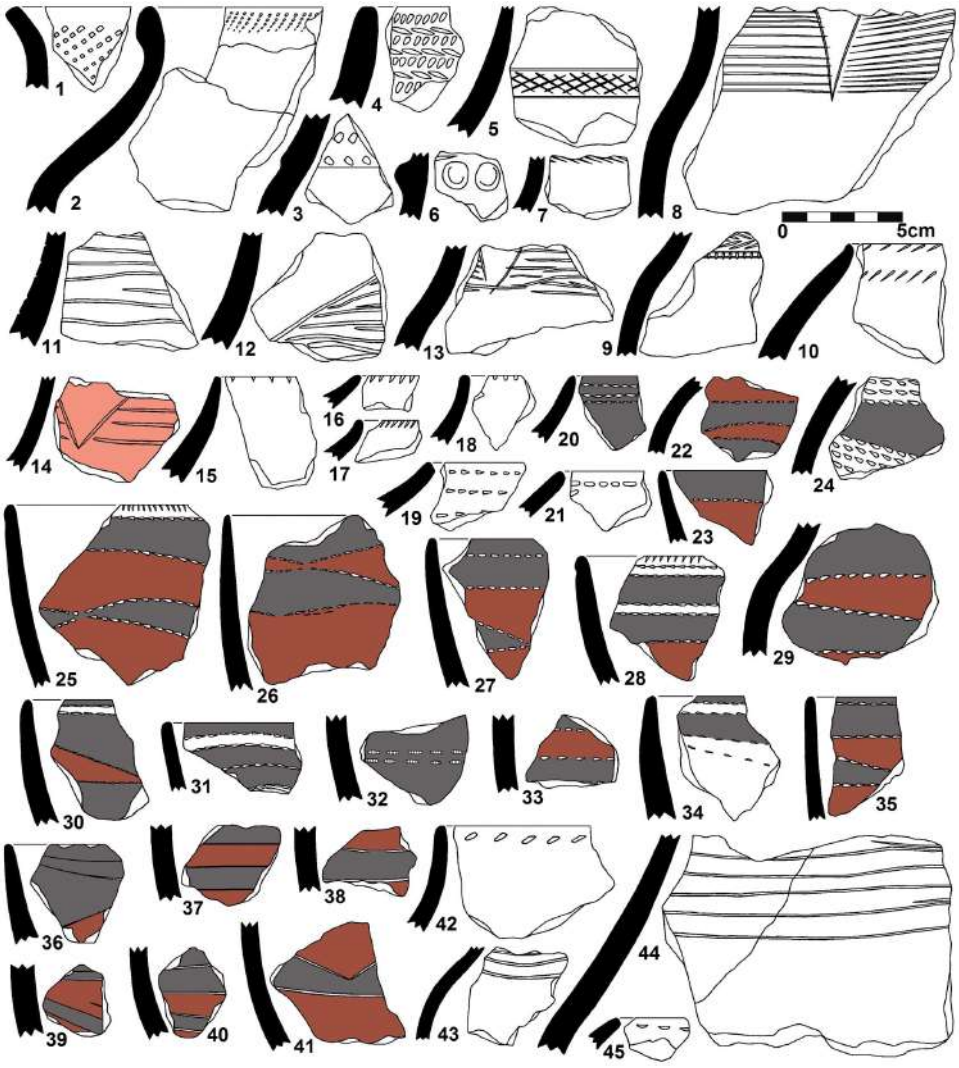

Fig. 14. Red Balloon Rock Shelter decorated ceramics retrieved during the surface collection. 1–3: Happy Rest facies; 4: Diamant facies; 5–9: Eiland facies; 10: Letsibogo facies; 11–14: Eiland facies; 15–42: Letsibogo facies; 43–44: Eiland facies; 45: Letsibogo facies.

bands of a smectite-type clay (Shillito et al. 2009; Müller et al. 2014). Bands of adsorbed water at 1647 (O-H bending) and 3308 (O-H stretching) cm^{-1} are also present. The weak feature at 744 cm^{-1} is attributed to feldspar, commonly found in association with clay (Vahur et al. 2016). There is no clear band of calcite on the spectrum of the Eiland 2 pottery sherd, but it could well be hidden behind the characteristic bands of organic matter between 1348 (C-H stretching due to amide, proteins) and 1406 (C-N stretching, proteins) cm^{-1} (Salman et al. 2010). The presence of organic matter is confirmed by the presence of weak features at 1592 (C-N stretching due to amide, proteins), 1744 (C-O stretching of carboxylic acid, lipids), 2855 (C-H stretching vibration due to CH3,

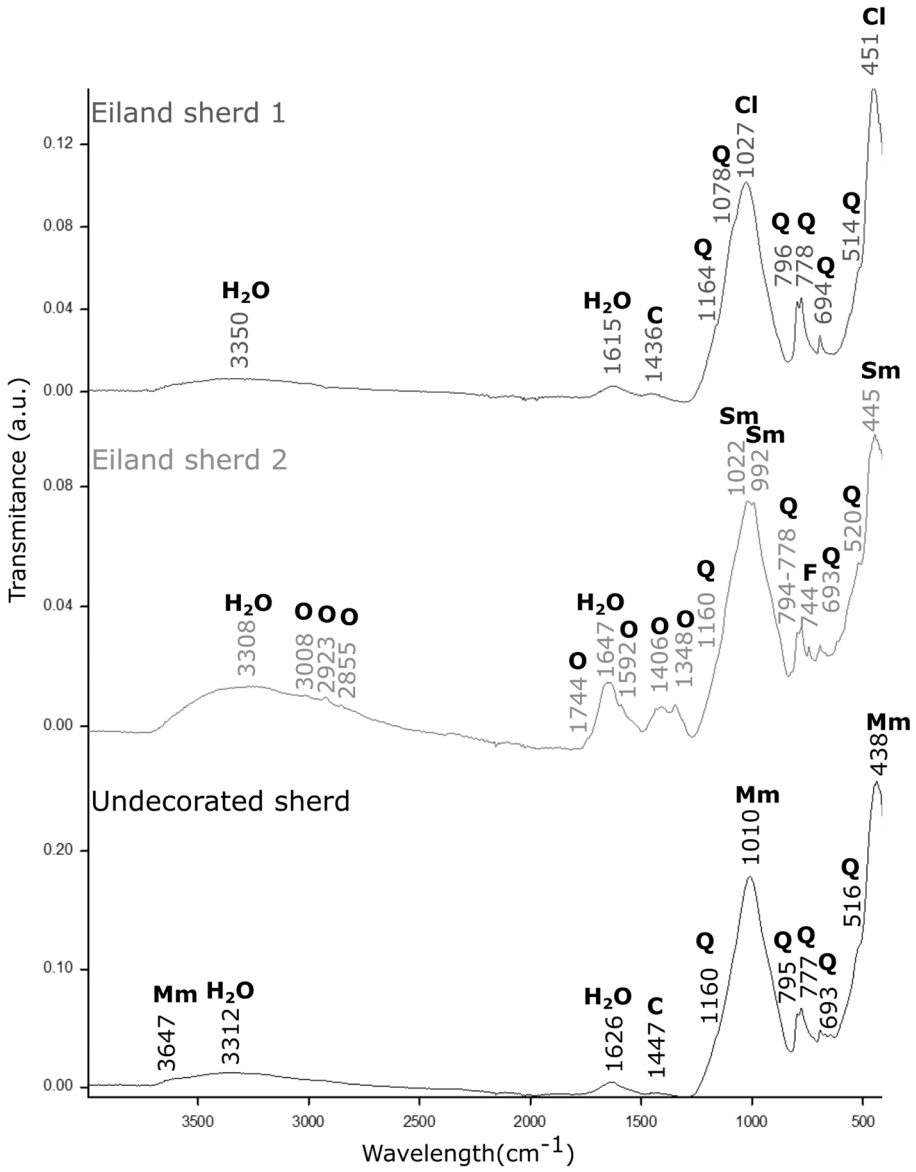

Fig. 15. FTIR spectra of three Red Balloon Rock Shelter ceramic sherds. C = calcite; Cl = unidentified clay; F = feldspar; Mm = montmorillonite clay; O = organic matter; Q = quartz; Sm = smectite clay.

lipids), 2923 (C-H stretching vibration due to CH2, lipids) and 3008 (C-H stretching due to lipids) cm^{-1} (Colombini et al. 2005; Salman et al. 2010). The detection of bands characteristic of lipids, proteins and unsaturated fatty acid support the hypothesis of adsorbed organic residue in the Eiland 2 pottery sherd. Spectra collected on the third ceramic specimen, the undecorated sherd, exhibit strong bands characteristic of clay, possibly montmorillonite at 438 (Si-O bending) and 1010 (Si-O stretching) cm^{-1}, with a weak feature at 3647 (Al–OH–Al stretching) cm^{-1} (Müller et al. 2014). Calcite was

detected at 1447 (carbonate asymmetric stretch) cm^{-1}, and adsorbed water at 1626 (O-H bending) and 3312 (O-H stretching) cm^{-1} (Shillito et al. 2009; Müller et al. 2014).

Beads, bead manufacture and bone points

Beads in a wide range of sizes were recovered from the Iron Age layers (Fig. 16). The inclusion of rough-outs and drilled fragments of ostrich eggshell (Table 12) points to the manufacture of at least some beads in Red Balloon Rock Shelter. While there is always the possibility that hunter-gatherers made some use of the shelter, there is no convincing evidence for LSA occupation here based on the lithic assemblage, although a single 'thumbnail' scraper was found in layer Dark Yellowish Brown. The ostrich eggshell beads may thus have been made by the Iron Age occupants of the shelter. Small beads are traditionally considered to have been made by hunter-gatherers while larger ones are thought to have been the handiwork of herders, yet Miller and Sawchuk (2019) demonstrate that small and larger beads co-occur throughout the Holocene in southern Africa. With a few exceptions (Fig. 16), the Red Balloon Rock Shelter beads are small (<3 mm diameter). They were mostly manufactured by drilling a hole through a square of shell, and thereafter shaping the bead. In most, but not all cases, the bead holes were drilled from one face of the shell only. Some of the beads have the cortex of dimpled pores removed from the surface of the eggshell, and grinding marks are occasionally evident on the surface of the beads. Where beads have been burnt it is not possible to see these grinding marks. One ostrich eggshell pendant was found in layer Dark Reddish Grey (#209). Snail shell (e.g. *Achatina* sp. shell) was used to produce thin beads and these can sometimes be recognised by the laminations visible on the rounded sides of the beads. There are also a few putative bone beads. Two broken bone points and one whole one were recovered (Fig. 16).

DISCUSSION

Red Balloon Rock Shelter may first have been occupied at about 104 ka ago and may have been abandoned by about 91 ka ago. OSL cannot, however, provide fine resolution, so the three age estimates presented here are unable to provide the exact duration of MSA occupation at the site, even though the ages are stratigraphically consistent. For this reason, the three age estimates were used to obtain a weighted mean age estimate of 96±4 ka ago for the MSA at Red Balloon Rock Shelter, intimating that the most likely occupation in the shelter was sometime during the period 100–92 ka ago.

A more detailed technological study of the Red Balloon Rock Shelter MSA lithics by Paloma de la Peña will follow in the future, so the observations here are preliminary ones. The large assemblage of bipolar cores at Red Balloon Rock Shelter is worthy of comment, particularly because Mason (1962: 273) observed that the *outil écaillé* class is well represented in Bed 2 of Olieboomspoort, but not in MSA assemblages farther east, like Cave of Hearths or Mwulu's Cave. Since Olieboomspoort and Red Balloon Rock Shelter are relatively close to each other, it is possible that this expedient method of working minerals like quartz was a local tradition in Marine Isotope Stage 5c–5b (approximately 106–84 ka ago). The age of the Red Balloon Rock Shelter assemblage makes it clear that bipolar knapping is integral to MSA technology. Thus, even large frequencies of bipolar knapping cannot be used as an attribute that exclusively characterises early LSA assemblages. Bipolar knapping was also reported at Kudu

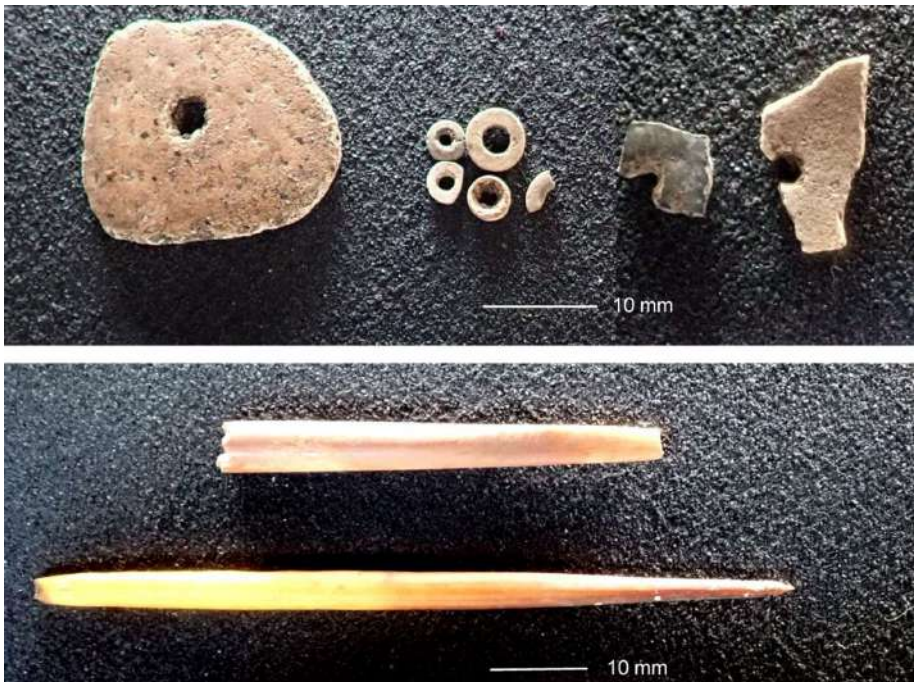

Fig. 16. Red Balloon Rock Shelter ostrich eggshell and bone points. Above: pendant, beads and bead manufacturing debris; below: bone point fragment and entire bone point.

Koppie in the Limpopo Valley (Wilkins 2008; Sumner 2013) and a great deal of bipolar knapping on both quartz and quartzite took place much later (~62–~58 ka ago) in the MSA at Sibudu (De la Peña & Wadley 2017).

Bipolar working is not the only feature of Red Balloon Rock Shelter technology recognised on the small river-rolled cobbles, because quartz, and sometimes quartzite cobbles, were exploited in several ways. Every now and then a cobble was simply opened to create a sharp edge that was then trimmed either as a scraper or denticulate. This simple but effective technique was evidenced also at Kudu Koppie, farther north near the Limpopo River, where it was used in the final ESA (Sangoan) (Wilkins 2008; Sumner 2013).

As mentioned in the introduction, archaeologists excavating MSA sites in the interior of South Africa, from the 1950s onwards, named assemblages with long blades and unifacial points Pietersburg Industries. These were recognised in Limpopo Province, but not north of the Limpopo River, and most were found in caves or rock shelters because such places attract explorers. Over time, almost any MSA lithic assemblage in Limpopo was called Pietersburg, regardless of its contents, so the model needs review (De la Peña et al. 2018). Olieboomspoort has, of course, been mentioned already, but the best known of the other so-called Pietersburg sites is Cave of Hearths, and other important ones are Bushman Rock Shelter near Ohrigstad, and Mwulu's Cave not far from the Makapan Valley. The hornfels-dominated assemblages from Bushman Rock Shelter have long blades, retouched blades, snapped and retouched sections of blades, and unifacial points (Volman 1981), and, in this regard, are completely different in

appearance from the Red Balloon Rock Shelter assemblage. Apart from the distinct technique of using snapped blades, these lithics were mostly made on locally available rocks that occur in sizeable chunks to enable striking large products; thus, the presence of long end-products may be a response to the availability of suitable, fine-grained rocks. Although obtaining chronology at Mwulu's Cave was difficult, the age of 90 ka ago seems appropriate (Feathers et al. 2020), therefore making this site more or less contemporary with Red Balloon Rock Shelter, and also with the oldest of the uppermost MSA layers at Bushman Rock Shelter, which have generated new OSL dates between 90 and 70 ka ago in layers where Levallois points are uncommon (Porraz et al. 2015, 2018). Mwulu's Cave was excavated in 1947 by Tobias (1949) and it was subsequently re-excavated by De la Peña and colleagues (2018). Mwulu's Cave has both Levallois flake and blade production, mostly on quartzite, and Levallois points are the most abundant tool type in the lower layers, while cores often show centripetal scar removals that are typical of Levallois-like reduction (De la Peña et al. 2018). The main retouched pieces at Mwulu's Cave are side-scrapers, notches and denticulates, and although a few bifacial pieces were found in the Tobias excavation, none was recently excavated (De la Peña et al. 2018). Levallois technological characteristics can also be seen in the deepest layers of Bushman Rock Shelter and Border Cave (Mason 1957; Sampson 1972, 1974; Beaumont 1978; Grün et al. 2003; Porraz et al. 2018). Tobias thought that there were resemblances between the lithics from Mwulu's Cave and Border Cave (Cooke et al. 1945), thus the Pietersburg label has been used there too (Beaumont 1978), even though, with hindsight, we know that a 90 ka occupation is not represented because Member 4WA is older than 115 ka ago (Grün et al. 2003).

The long hiatus between the MSA and the Iron Age at Red Balloon Rock Shelter is part of the conundrum that Van der Ryst (1998) drew attention to at other Waterberg plateau sites. Since the hiatus is not geologically marked, Red Balloon Rock Shelter cannot contribute to solving the puzzle. Hyrax middens present in some of the adjacent rock shelters provide some hope that an independent environmental record can, in the future, be obtained for at least the last 50 000 years (at the outer limit of AMS radiocarbon dating). Elsewhere in southern Africa, hyrax middens have provided detailed environmental records (e.g. Chase et al. 2011). It is not impossible that the Waterberg plateau experienced exceedingly wet conditions towards the end of Marine Isotope Stage 5. When there is heavy or protracted rain in the Waterberg, water runs from cracks in the rocks (this is the derivation of the mountain range's name) and open plains or valleys can quickly become soggy wetlands, teeming with mosquitoes. Although Red Balloon is now a dry shelter, this may not have been the case in Marine Isotope Stage 5, as implied by the dried mud that is deposited on its MSA lithics.

Red Balloon Rock Shelter's seed identifications and our survey of the vegetation in the surrounding area suggest that the environment near the shelter has been essentially the same over the past 200 years. Our record of the modern vegetation was made before the new summer growth on the deciduous taxa and we are consequently likely to have overlooked some trees and shrubs. This explains the absence in the modern tree list of some taxa present in the archaeobotanical assemblage. Apart from the windblown grass, Asclepiad-type and Asteraceae seeds, the other seeds are edible and could easily have been brought into the shelter by animals and birds. If birds or animals ate the red balloon (*E. transvaalensis*) seeds for their oil, one would not expect to find them

whole. Whole red balloon seeds were recovered and this may imply an anthropogenic origin for the seeds, perhaps for use as beads. Since other types of beads were found in the shelter, this suggestion is not improbable. The lack of organic preservation in the MSA prevents any interpretation about the time depth of people's possible use of red balloon seeds. No vegetation change or definitive evidence of anthropogenic agency in the any of the seed and fruit taxa was identified.

The Red Balloon Rock Shelter occupation hiatus was broken when pastoralists (Sadr 2015) or Iron Age agropastoralists first moved to the uplands (Van der Ryst 1998; Huffman 2007). The presence of decorated sherds representing a range of ceramic facies points towards the use of the shelter from early in the pastoral and/or Iron Age narrative in Limpopo. Since there is no evidence that these people lived in the shelter until it may have become a desirable refuge from violence about 200 years ago, it seems most likely that early use of the shelter was for ritual purposes, rain-making being amongst these. The ritual probably involved leaving gifts for ancestors, for example, pots with herbal medicine. Beads may have been gifted, too, and some of the ostrich eggshell beads may have been obtained through exchange with San, though others appear to have been made in the shelter by the agropastoralists, as evidenced by shell debris with manufacturing marks found in the ash of the hearth feature. They cover a range of sizes from extremely small to much larger, and there are also a few snail shell beads. Ostrich are not suited to the plateau conditions, and the eggshell, and perhaps some of the beads themselves, are likely to have come from below the plateau. A single pale-blue glass bead was also recovered. These beads were first made in Venice in the early 19th century (Wood 2000, 2008). Around that time, bead-makers started to use synthetic colourants to tint the glass. Arsenic was added to whitish glass to make it chalk white. Cobalt blue was added to the white to make pale-blue glass. The earliest dates in South Africa for these beads come from uMgungundlovu, capital of the Zulu kingdom between AD 1829 and 1838 (Wood 2008). In Limpopo they have been found at Makapan and Maleoskop dating to around AD 1850 (Wood 2008), so they could only have arrived in Red Balloon Rock Shelter after AD 1830.

The group that camped in the shelter, probably during the *difaqane,* made at least one large hearth towards the back of the shelter, and also buried and burned rubbish in a pit, perhaps as part of the attempt to detract (human and animal) attention from their presence there. Small animals were consumed in the shelter, including some of sheep/goat/impala size. Stone walling adjacent to one of the neighbouring rock shelters suggests that a few domestic animals were hidden on the hill, too, but that they were housed separately from people. The excavated Iron Age material was all recent, yet the surface of the shelter has many decorated sherds from earlier ceramic facies including Happy Rest and Eiland. The different FTIR bands attributed to the clays support the idea that the ceramics were made from at least three distinct clays. Further analyses could investigate their firing temperatures, because this information would be useful for determining the techniques used to produce them (Lindahl & Pikirayi 2010; Damm 2012). Nonetheless, our preliminary analysis showing that different clay types were selected through time, may point to the use of distinct ceramic production techniques. It also points to the presence of organic residue on one Eiland pottery sherd, most certainly due to its use as a container for organic products. The placing of gifts for ancestors in rock crevices explains the presence of much of the pottery,

and the continued use of the shelter by leopard, hyena and other animals has caused redistribution and fragmentation of ceramics.

Agropastoralists relied heavily on adequate rainfall for the cultivation of their crops and for watering their livestock. To control the rainfall and timing thereof, chiefs and rainmakers had to execute certain ceremonies and rituals that differed between communities (Schoeman 2006). Ethnographic accounts, for example by Schapera (1930) and Feddema (1966) amongst Tswana communities, highlight the importance of rain-control rituals. As rain controllers, Tswana chiefs kept the tools and pots used for these rituals in their rain enclosures. For example, Lentswe's (Kgatla chief AD 1874–1920) rain enclosure was a small rock shelter located at the back of his mother's quarters on Phuthadikobo Hill in Mochudi, Botswana, about 150 km from Red Balloon Rock Shelter. Other ethnographic data (Schapera 1930; Feddema 1966) also indicate that caves and shelters played a central role in Tswana rain-control ceremonies. As Moloko pottery (in the form of Letsibogo) is the facies most commonly found in the Red Balloon Rock Shelter collection, we suggest that the shelter was used in rain-control rituals by Tswana groups in the region.

Numerous Letsibogo facies sites dating from the 16th century onward were recorded to the west of the Waterberg and adjacent in Botswana (Biemond 2014). Madikwe facies sites dating from the 16th century onward were documented in the Thabazimbi and Rooiberg area (Hall 1981; Huffman 2006). Letsibogo and Madikwe facies pottery was absent in the Olieboomspoort collection, although it had some 'Icon' type vessels. The abundance of the Icon pottery seems to be associated with rituals, as is attested by the ochre-stained bowls. The 'late white' rock art at Olieboomspoort can probably be linked to the Late Iron Age use of the shelter (and thus also to the probable makers of Icon pottery) (see Van der Ryst 2006). We can argue that the white paintings in shelters (Laue 2001) adjacent to Red Balloon Rock Shelter imply Late Iron Age ritual there, too. Thus, the Moloko ceramics in the shelter point towards their ritual use in the Iron Age.

During the *difaqane* many people hid in the mountains, with small groups taking refuge in narrow valleys, rock shelters and caves in remote parts of the Waterberg mountains. The pioneer traveller Dr Andrew Smith passed through the region in September 1835 (Lye 1975: 264–274). He encountered 'poor Baquan' (Bakwena) who could not continue planting crops along the Limpopo as formerly (Kirby 1940: 203) due to regular raiding by the Matebele (Ndebele) of Mzilikazi. Within this *difaqane* context, a small group of people, probably poor Bakwena, likely sought refuge in Red Balloon Rock Shelter and left the undecorated pottery that was excavated around at least one large hearth towards the back of the shelter. As mentioned earlier, these inhabitants also buried and burned rubbish in a pit.

The pattern of occupation at Red Balloon Rock Shelter follows that observed elsewhere on the high plateau by Van der Ryst (2006), namely, MSA occupation followed by a hiatus that ends with recent agropastoralist occupation. Red Balloon Rock Shelter's OSL ages are the first MSA age estimates for the plateau, so we cannot comment on whether they represent MSA chronology at other plateau sites. We now know that the occupation hiatus is considerable; however, we are no closer than Van der Ryst to explaining why the hiatus exists. We suspect an environmental cause, and the clay-coated MSA lithics imply waterlogged conditions, but for the moment we are

unable to test the hypothesis and we await the opportunity to sample material that can provide independent environmental information.

ACKNOWLEDGEMENTS

Lyn Wadley acknowledges the support of the Evolutionary Studies Institute at the University of the Witwatersrand (Wits). We thank the Wits School of Geography, Archaeology and Environmental Studies (GAES) for the loan of the Nikon Nivo 5C and Prof. D. Stratford for instruction on its use. The manager of the farm on which Red Balloon is situated is thanked for assistance in many ways. We abide by the owners' request to keep the name of the property and principals private. Red Balloon was excavated with SAHRA permit #15121. We thank Dr S. Woodborne of iThemba Labs for the radiocarbon date, and Dr Terry Lachlan and Dr Lili Yu for assistance in the Wollongong OSL dating laboratory. We are grateful to two anonymous reviewers for suggestions that improved the paper.

REFERENCES

Aukema, J. 1989. Rain-making: a thousand year-old ritual? *South African Archaeological Bulletin* **44**: 70–2.

Backwell, L., McCarthy, T.S., Wadley, L., Henderson, Z., Steininger, C.M., De Klerk, B., Barré, M., Lamothe, M., Chase, B.M., Woodborne, S., Susino, G.J., Bamford, M.K., Sievers, C., Brink, J.S., Rossouw, L., Pollarolo, L., Trower, G., Scott, L. & d'Errico, F. 2014. Multiproxy record of late Quaternary climate change and Middle Stone Age human occupation at Wonderkrater, South Africa. *Quaternary Science Reviews* **99**: 42–59.

Barré, M., Lamothe, M., Backwell, L. & McCarthy, T. 2012. Optical dating of quartz and feldspars: a comparative study from Wonderkrater, a Middle Stone Age site of South Africa. *Quaternary Geochronology* **10**: 374–9.

Beaumont, P.B. 1978. *Border Cave*. MA dissertation, University of Cape Town.

Biemond, W.M. 2014. *The Iron Age sequence around a Limpopo river floodplain on Basinghall Farm, Tuli Block, Botswana, during the second millennium AD*. MA dissertation, University of South Africa.

Boeyens, J., Van der Ryst, M., Coetzee, F., Steyn, M. & Loots, M. 2009. From uterus to jar: the significance of an infant pot burial from Melora Saddle, an early nineteenth-century African farmer site on the Waterberg Plateau. *Southern African Humanities* **21**: 213–38.

Boeyens, J. & Van der Ryst, M. 2014. The cultural and symbolic significance of the African rhinoceros: a review of the traditional beliefs, perceptions and practices of agropastoralist societies in southern Africa. *Southern African Humanities* **26**: 21–55.

Bøtter-Jensen, L., Andersen, C.E., Duller, G.A.T. & Murray, A.S. 2003. Developments in radiation, stimulation and observation facilities in luminescence measurements. *Radiation Measurements* **37**: 535–41.

Bøtter-Jensen, L., Bulur, E., Duller, G.A.T. & Murray, A.S. 2000. Advances in luminescence instrument systems. *Radiation Measurements* **32**: 523–8.

Brennan, B.J. 2003. Beta doses to spherical grains. *Radiation Measurements* **37**: 299–303.

Chase, B.M., Quick, L.J., Meadows, M.E., Scott, L., Thomas, D.S.G. & Reimers, P.J. 2011. Late glacial interhemispheric climate dynamics revealed in South African hyrax middens. *Geology* **39**: 19–22.

Colombini, M.P., Giachi, G., Modugno, F. & Ribechini, E. 2005. Characterisation of organic residues in pottery vessels of the Roman age from Antinoe (Egypt). *Microchemical Journal* **79** (1–2): 83–90.

Cooke, H.B.S., Malan, B.D. & Wells, L.H. 1945. Fossil man in the Lebombo Mountains, South Africa. *Man* **3**: 6–12.

Damm, C.B. 2012. From entities to interaction: replacing pots and people with networks of transmission. In R. Grünthal & P. Kallio (eds), *A linguistic map of northern Europe*. Helsinki: Mémoires de la Societé Finno-Ougrienne 266, pp. 41–62.

De Bruiyn, H. 1971. The geology of the central portion of the Waterberg basin around Vaalwater, Northern Transvaal. Unpublished report of the Geological Survey of South Africa, 1971-0044: 1–11.

Delius, P. 1983. *The land belongs to us: the Pedi Polity, the Boers and the British in the nineteenth-century Transvaal*. Ravan Press: Johannesburg.

De la Peña, P., Val, A., Stratford, D.J., Colino, F., Esteban, I., Fitchett, J.M., Hodgskiss, T., Matembo, J. & Moll, R. 2018. Revisiting Mwulu's Cave: new insights into the Middle Stone Age in the southern African savanna biome. *Archaeological and Anthropological Sciences*: **11**: 3239–66.

De la Peña, P. & Wadley, L. 2017. Technological variability at Sibudu Cave: the end of Howiesons Poort and reduced mobility strategies after 62,000 years ago. *PLoS ONE* **12**: article 10, 41 pp.

De la Peña, P. & Witelson, D. 2018. Trampling vs. retouch in a lithic assemblage: a case study from a Middle Stone Age site Steenbokfontein 9KR (Limpopo, South Africa). *Journal of Field Archaeology* **43**: 522–37.

De Vries, W.C.P. 1970. Stratigraphy of the Waterberg System in the southern Waterberg area, northwestern Transvaal. *Annals of the Geological Survey of South Africa* **7**: 43–67.

De Vries, W.C.P. 1973. Sedimentary structures in the southern and central portions of the Waterberg area, northwestern Transvaal. *Geologie en Mijnbouw* **52**: 133–40.

Feathers, J.K., Evans, M., Stratford, D.J. & De la Peña, P. 2020. Exploring complexity in luminescence dating of quartz and feldspars at the Middle Stone Age site of Mwulu's Cave (Limpopo, South Africa). *Quaternary Geochronology* **59**: article 101092, 16 pp.

Feddema, J.P. 1966. Tswana ritual concerning rain. *African Studies* **25** (4): 181–95.

Forssman, T. 2020. *Foragers in the middle Limpopo Valley: trade, place-making and social complexity*. Cambridge Monographs in African Archaeology 100. Oxford: Archaeopress.

Galbraith, R.F., Roberts, R.G., Laslett, G.M., Yoshida, H. & Olley, J.M. 1999. Optical dating of single and multiple grains of quartz from Jinmium rock shelter, northern Australia, part 1, experimental design and statistical models. *Archaeometry* **41**: 339–64.

Goodwin, A.J.H. & Van Riet Lowe, C. 1929. The Stone Age cultures of South Africa. *Annals of the South African Museum* **27**: 1–289.

Grün, R., Beaumont, P.B., Tobias, P.V. & Eggins, S. 2003. On the age of Border Cave 5 human mandible. *Journal of Human Evolution* **45**: 155–67.

Guérin, G., Mercier, N. & Adamiec, G. 2011. Dose-rate conversion factors: update. *Ancient TL* **29**: 5–8.

Guo, Y., Li, B. & Zhao, H. 2020. Comparison of single-aliquot and single-grain MET-pIRIR D_e results for potassium feldspar samples from the Nihewan Basin, northern China. *Quaternary Geochronology* **56**: article 101040, 10 pp.

Guralnik, B., Li, B., Jain, M., Chen, R., Paris, R.B., Murray, A.S., Li, S.-H., Pagonis, V., Valla, P.G. & Herman, F. 2015. Radiation-induced growth and isothermal decay of infrared-stimulated luminescence from feldspar. *Radiation Measurements* **81**: 224–31.

Hall, S.L. 1981. *Iron Age sequence and settlement in the Rooiberg, Thabazimbi area*. MA dissertation, University of the Witwatersrand.

Hankey, A. 2004. *Pappea capensis* Eckl. & Zeyh. PlantzAfrica. <http://pza.sanbi.org/pappea-capensis>; site viewed 27 February 2021.

Hublin, J.-J., Ben-Ncer, A., Bailey, S.E., Freidline, S.E., Neubauer, S., Skinner, M.M., Bergmann, I., Le Cabec, A., Bennazi, S., Harvati, K. & Gunz, P. 2017. New fossils from Jebel Irhoud, Morocco and the pan-African origin of Homo sapiens. *Nature* **546**: 289–92.

Huffman, T.N. 1990. Obituary: The Waterberg research of Jan Aukema. *South African Archaeological Bulletin* **45**: 117–9.

Huffman, T.N. 2006. Maize grindstones, Madikwe pottery and ochre mining in pre-colonial South Africa. *Southern African Humanities* **18**: 51–70.

Huffman, T.N. 2007. *Handbook to the Iron Age: the archaeology of pre-colonial farming societies in southern Africa*. Pietermaritzburg: University of KwaZulu-Natal Press.

Hutson, J.M. & Cain, C.R. 2008. Reanalysis and reinterpretation of the Kalkbank faunal accumulation, Limpopo Province, South Africa. *Journal of Taphonomy* **6**: 399–428.

Jacobs, Z., Li, B., Shunkov, M.V., Kozlikin, M.B., Bolikhovskaya, N.S., Agadjanian, A.K., Uliyanov, V.A., Vasiliev, S.K., O'Gorman, K., Derevianko, A.P. & Roberts, R.G. 2019. Timing of archaic hominin occupation of Denisova Cave in southern Siberia. *Nature* **565**: 594–9.

Jansen, H. 1982. The geology of the Waterberg Basins in the Transvaal, Republic of South Africa. *Geological Survey Memoir* **71**: 1–98.

Kirby, P.C. (ed.) 1940. *The diary of Dr Andrew Smith, 1834–1836*. Vol. 2. Cape Town: Van Riebeeck Society.

Kreutzer, S., Schmidt, C., Fuchs, M.C., Dietze, M., Fischer, M. & Fuchs, M. 2012. Introducing an R package for luminescence dating analysis. *Ancient TL* **30**: 1–8.

Kuman, K., Gibbon, R., Kempson, H., Langejans, G., Le Baron, J.C., Pollarolo L. & Sutton, M. 2005. Stone Age signatures in northernmost South Africa: early archaeology in the Mapungubwe National

Park and vicinity. In F. d'Errico & L. Backwell (eds), *From tools to symbols, from early hominids to modern humans*. Johannesburg: Witwatersrand University Press, pp. 163–82.

Laue, G.B. 2001. The Rock Art of Kurumakatiti Game Reserve. Report in the Rock Art Research Institute, University of the Witwatersrand.

Le Baron, J.C., Kuman, K. & Grab, S.W. 2010. The landscape distribution of Stone Age artefacts on the Hackthorne Plateau, Limpopo River Valley, South Africa. *South African Archaeological Bulletin* **68**: 123–31.

Li, B., Jacobs, Z. & Roberts, R.G. 2016. Investigation of the applicability of standardised growth curves for OSL dating of quartz from Haua Fteah cave, Libya. *Quaternary Geochronology* **35**: 1–15.

Li, B., Jacobs, Z. & Roberts, R.G. 2020. Validation of the LnTn method for De determination in optical dating of K-feldspar and quartz. *Quaternary Geochronology* **58**: article 101060, 14 pp.

Li, B., Jacobs, Z., Roberts, R.G., Galbraith, R. & Peng, J. 2017. Variability in quartz OSL signals caused by measurement uncertainties: problems and solutions. *Quaternary Geochronology* **41**: 11–25.

Li, B. & Li, S.-H. 2012. A reply to the comments by Thomsen et al. on 'Luminescence dating of K-feldspar from sediments: A protocol without anomalous fading correction'. *Quaternary Geochronology* **8**: 49–51.

Li, B., Roberts, R.G., Jacobs, Z. & Li, S.-H. 2015a. Potential of establishing a 'global standardised growth curve' (gSGC) for optical dating of quartz from sediments. *Quaternary Geochronology* **27**: 94–104.

Li, B., Roberts, R.G., Jacobs, Z., Li, S.-H. & Guo, Y.J. 2015b. Construction of a 'global standardised growth curve' (gSGC) for infrared stimulated luminescence dating of K-feldspar. *Quaternary Geochronology* **27**: 119–30.

Lindahl, A. & Pikirayi, I. 2010. Ceramics and change: an overview of pottery production techniques in northern South Africa and eastern Zimbabwe during the first and second millennium AD. *Archaeological and Anthropological Sciences* **2** (3): 133–49.

Lye, W.F. (ed.) 1975. *Andrew Smith's journal of his expedition into the interior of South Africa, 1834–1836*. Cape Town: Balkema.

Mason, R.J. 1951. Excavation of four caves near Johannesburg. *South African Archaeological Bulletin* **6**: 71–9.

Mason, R.J. 1957. The Transvaal Middle Stone Age and statistical analysis. *South African Archaeological Bulletin* **12**: 119–43.

Mason, R.J. 1962. *Prehistory of the Transvaal*. Johannesburg: Witwatersrand University Press.

Mason, R.J. 1988. *Cave of Hearths, Makapansgat, Transvaal*. Johannesburg: University of the Witwatersrand Archaeological Research Unit Occasional Paper 21.

Miller, J.M. & Sawchuk, E.A. 2019. Ostrich eggshell bead diameter in the Holocene: regional variation with the spread of herding in eastern and southern Africa. *PLoS ONE* **14**: article 11, 19 pp.

Müller, C.M., Pejcic, B., Esteban, L., Delle Piane, C., Raven, M. & Mizaikoff, B. 2014. Infrared attenuated total reflectance spectroscopy: an innovative strategy for analyzing mineral components in energy relevant systems. *Scientific Reports* **4** (1): 1–11.

Nathan, R.P. & Mauz, B. 2008. On the dose-rate estimate of carbonate-rich sediments for trapped charge dating. *Radiation Measurements* **43**: 14–25.

Palmer, E. & Pitman, N. 1972. *Trees of southern Africa*. Vol. 2. Cape Town: Balkema.

Peng, J., Dong, Z., Han, F., Long, H. & Liu, X. 2013. R package numOSL: numeric routines for optically stimulated luminescence dating. *Ancient TL* **31**: 41–8.

Peng, J. & Li, B. 2017. Single-aliquot regenerative-dose (SAR) and standardised growth curve (SGC) equivalent dose determination in a batch model using the R Package 'numOSL'. *Ancient TL* **35**: 32–53.

Pike, A.W.G., Eggins, S., Grün, R. & Thackeray, F. 2004. U-series dating of TP1, an almost complete human skeleton from Tuinplaas (Springbok Flats), South Africa. *South African Journal of Science* **100**: 381–3.

Plug, I. 1981. Some research results on the late Pleistocene and early Holocene deposits of Bushman Rock Shelter, eastern Transvaal. *South African Archaeological Bulletin* **36**: 14–21.

Pollarolo, L. & Kuman, K. 2009. Excavation at Kudu Koppie: a Stone Age site in Limpopo Province, South Africa. *South African Archaeological Bulletin* **64**: 69–74.

Porraz, G., Val, A., Dayet, L., De la Peña, P., Douze, K., Miller, C., Murungi, M., Tribolo, C., Schmid, V. & Sievers, C. 2015. Bushman Rock Shelter (Limpopo, South Africa): a perspective from the edge of the Highveld. *South African Archaeological Bulletin* **70**: 166–79.

Porraz G., Val, A., Tribolo, C., Mercier, N., De la Peña, P., Haaland, M., Igreja, M., Miller, K. & Schmid, V. 2018. The MIS5 Pietersburg at '28' Bushman Rock Shelter, Limpopo Province, South Africa. *PloS One* **13**: article 10, 45 pp.

Prescott, J.R. & Hutton, J.T. 1994. Cosmic-ray contributions to dose rates for luminescence and ESR dating: large depths and long-term time variations. *Radiation Measurements* **23**: 497–500.

Reimann, T., Thomsen, K.J., Jain, M., Murray, A.S. & Frechen, M. 2012. Single-grain dating of young sediments using the pIRIR signal from feldspar. *Quaternary Geochronology* **11**: 28–41.

Rousseeuw, P.J., Debruyne, M., Engelen, S. & Hubert, M. 2006. Robustness and outlier detection in chemometrics. *Critical Reviews in Analytical Chemistry* **36**: 221–42.

Sadr, K. 2015. Livestock first reached southern Africa in two separate events. *PLoS ONE* **10**: article 8, 22 pp.

Salman, A., Tsror, L., Pomerantz, A., Moreh, R., Mordechai, S. & Huleihel, M. 2010. FTIR spectroscopy for detection and identification of fungal phytopathogenes. *Spectroscopy* **24** (3–4): 261–7.

Sampson, C.G. 1972. *The Stone Age Industries of the Orange River Scheme and South Africa*. Bloemfontein: National Museum Memoir 6.

Sampson, C.G. 1974. *The Stone Age archaeology of southern Africa*. New York: Academic Press.

Schapera, I. 1930. The 'little rain' (*pulanyana*) ceremony of Bechuanaland baKxatla. *Bantu Studies* **4**: 211–6.

Schoeman, M.H. 2006. *Clouding power? Rain control space, landscapes and ideology*. PhD thesis, University of the Witwatersrand.

Schoonraad, M. & Beaumont, P.B. 1968. The North Brabant Shelter, north western Transvaal. *South African Journal of Science* **64**: 319–31.

Shillito, L.M., Almond, M.J., Nicholson, J., Pantos, M. & Matthews, W. 2009. Rapid characterisation of archaeological midden components using FT-IR spectroscopy, SEM–EDX and micro-XRD. *Spectrochimica Acta Part A: Molecular and Biomolecular Spectroscopy* **73** (1): 133–9.

Sinclair, A. 2009. The MSA stone tool assemblage from the Cave of Hearths, Beds 4–9. In J. McNabb & A. Sinclair (eds), *The Cave of Hearths: Makapan Middle Pleistocene Research Project: field research by Anthony Sinclair and Patrick Quinney, 1996–2001*. Oxford: Archaeopress, pp. 105−37.

South African National Biodiversity Institute. 2016. Botanical Database of Southern Africa (BODATSA) [dataset]. http://posa.sanbi.org/sanbi/Explore; site viewed 27 August 2021.

Sumner, T.A. 2013. A refitting study of late Early to Middle Stone Age lithic assemblages from the site of Kudu Koppie, Limpopo Province, South Africa. *Journal of African Archaeology* **11**: 133−53.

Thomsen, K.J., Murray, A.S., Jain, M. & Bøtter-Jensen, L. 2008. Laboratory fading rates of various luminescence signals from feldspar-rich sediment extracts. *Radiation Measurements* **43**: 1474–86.

Tobias, P.V. 1949. The excavation of Mwulu's Cave, Potgietersrust district. *South African Archaeological Bulletin* **4**: 2–13.

Tobias, P.V. 1971. Human skeletal remains from the Cave of Hearths, Makapansgat, northern Transvaal. *American Journal of Physical Anthropology* **34**: 335–67.

Vahur, S., Teearu, A., Peets, P., Joosu, L. & Leito, I. 2016. ATR-FT-IR spectral collection of conservation materials in the extended region of 4000-80 cm^{-1}. *Analytical and Bioanalytical Chemistry* **408** (13): 3373–9.

Val, A., De la Peña, P., Duval, M., Bansal, S., Colino, F., Culey, J., Hodgskiss, T., Morrissey, P., Murray, A., Murungi, M., Neumann, F.H., Shadrach, K., Thomsen, K.J., Van der Ryst, M., Witelson, D.M., Zhao, J.X. & Stratford, D. 2021. The place beyond the trees: renewed excavations of the Middle Stone Age deposits at Olieboomspoort in the Waterberg Mountains of the South African Savanna Biome. *Archaeological and Anthropological Sciences* **13**: article 116, pp. 32.

Van der Ryst, M.M. 1998. *The Waterberg Plateau in the Northern Province, Republic of South Africa, in the Later Stone Age*. Oxford: British Archaeological Reports, International Series S715.

Van der Ryst, M.M. 2006. *Seeking shelter: Later Stone Age hunters, gatherers and fishers of Olieboomspoort in the western Waterberg, south of the Limpopo*. PhD thesis, University of the Witwatersrand.

Van Doornum, B.L. 2008. Sheltered from change: hunter-gatherer occupation of Balerno Main Shelter, Shashe-Limpopo confluence area, South Africa. *Southern African Humanities* **20**: 249–84.

Van Schalkwyk, J.A. 2000. Excavation of a Late Iron Age site in the Makgabeng, Northern Province. *Southern African Field Archaeology* **9**: 75–82.

Van Wyk, A.E., Winter, P.J.D., Hahn, N. & Von Staden, L. 2016. *Erythrophysa transvaalensis*. I. Verd. National Assessment, Red List of South African Plants version 2020.1. <http://redlist.sanbi.org/species.php?species=3855-2>; site viewed 27 February 2021.

Van Wyk, B. & Van Wyk, P. 2013. *Field guide to trees of southern Africa*. 2nd edition. Cape Town: Struik.

Voigt, W. 2010. *Erythrophysa alata* (Eckl. & Zeyh.) Hutch. PlantzAfrica. <http://pza.sanbi.org/erythrophysa-alata>; site viewed 14 April 2021.

Volman, T.P. 1981. *The Middle Stone Age in the southern Cape*. PhD thesis, University of Chicago.

Wadley, L., Murungi, M.L., Witelson, D., Bolhar, R., Bamford, M., Sievers, C., Val, A. & De la Peña, P. 2016. Steenbokfontein 9KR: A Middle Stone Age spring site in Limpopo, South Africa. *South African Archaeological Bulletin* **71**: 130–45.

Wilkins, J.R. 2008. *Prepared core reduction strategies at Kudu Koppie and the modern human behavior debate*. MA dissertation, University of Calgary.

Wintle, A.G. 1997. Luminescence dating: laboratory procedures and protocols. *Radiation Measurements* **27** (5–6): 769–817.

Wood, M. 2000. Making connections: relationships between international trade and glass beads from the Shashe-Limpopo area. *South African Archaeological Society Goodwin Series* **8**: 78–90.

Wood, M. 2005. *Glass beads and pre-European trade in the Shashe-Limpopo region*. MSc dissertation, University of the Witwatersrand.

Wood, M. 2008. Post-European contact glass beads from the southern African interior: a tentative look at trade, consumption and identities. In N. Swanepoel, A. Esterhuysen & P. Bonner (eds), *Five hundred years rediscovered: southern African precedents and prospects*. Johannesburg: Wits University Press, pp. 183–96, Plates 6–21.

Wood, M. 2011. *Interconnections: glass beads and trade in southern and eastern Africa and the Indian Ocean 7th to 16th centuries AD*. Uppsala, Sweden: Studies in Global Archaeology 17.

TABLE 1

Red Balloon Rock Shelter, Limpopo: preliminary tree and shrub list in the site's surrounds.

Scientific name	Common name (English/Afrikaans)
Acacia caffra, syn. for *Vachellia caffra*	common hook thorn, wag-'n-bietjiedoring
Acacia karroo, syn. for *Vachellia karroo*	sweet thorn, soetdoring
Acacia mellifera, syn. for *Senegalia mellifera*	black thorn, swarthaak
Acacia nilotica, syn. for *Vachellia nilotica*	scented-podthorn, lekkerruikpeul
Albizia tanganyicensis	paperbark false-thorn, papierbasvalsdoring
Berchemia zeyheri	red ivory, rooi ivoor
Boscia albitrunca	shepherd's tree, witgat
Brachylaena huillensis	lowveld silver-oak, laeveldvaalbos
Combretum zeyheri	large-fruited bushwillow, raasblaar
Commiphora marlothii	paperbark corkwood, papierbaskanniedood
Commiphora cf. *mollis*	velvet-leaved corkwood, fluweelkanniedood
Croton gratissimus	lavender feverberry, harige laventelkoorsbessie
Dichrostachys cinerea	sicklebush, sekelbos
Elaeodendron transvaalense	bushveld saffron, bosveldsaffraan
Erythrophysa transvaalensis	bushveld red balloon, bosveldrooiklapperbos
Euclea natalensis	bushveld hairy guarri, bosveld haarige ghwarrie
Ficus thonningii, syn. *Ficus burkei*	strangler fig, gewone wildevy
Ficus ingens	red-leaved fig, rooiblaarvy
Gardenia volkensii	bushveld gardenia, bosveldkatjiepiering
Grewia flava	velvet raisin, rosyntjiebos
Grewia flavescens	sandpaper raisin, skurweblaarrosyntjie
Heteropyxis natalensis	lavender tree, laventelboom
Mimusops zeyheri	common red-milkwood, moepel
Obetia tenax	mountain nettle, bergbrandnetel
Pappea capensis	jacketplum, doppruim
Pavetta eylesii	large-leaved bride's bush, grootblaarbruidsbos
Peltophorum africanum	African wattle, huilboom
Pterocarpus rotundifolius	round-leaved teak, dopperkiaat
Searsia leptodictya	mountain karee, bergkaree
Searsia sp.	-
Schotia brachypetala	weeping boerbean, huilboerboon
Sclerocarya birrea	marula, maroela
Spirostachys africana	tamboti, tambotie
Sterculia rogersii	star-chestnut, sterkastaiing
Ximenia caffra	sourplum, suurpruim
Ziziphus mucronata	buffalo-thorn, wag-'n-bietjie

TABLE 2

D_e measurement procedure for single-grain K-feldspar. [a] For the natural samples, D_i = 0 Gy (grain yield).

Step	Treatment
1	Give regenerative dose, D_i [a]
2	Preheat at 320 °C for 60 s
3	IR diodes stimulation at 200 °C for 200 s
4	Single-grain IR laser stimulation (2 s) at 275°C
5	Give test dose, D_t
6	Preheat at 320 °C for 60 s
7	IR diodes stimulation at 200 °C for 200 s
8	Single-grain IR laser stimulation (2 s) at 275°C
9	IR bleaching at 325 °C for 100 s
10	Return to step 1

TABLE 3

Red Balloon Rock Shelter strata: layer names, volume of sediment in litres, dating and attribution. Not all layers are present in both squares, or even across an entire square.

Layer name and number of sub-layers	Abbreviation	Volume litres D9	Volume litres E9	Total station #D9, #E9	Age	OSL#	Attribution
MSA layers							
Dark Olive Brown 1,2	DOB	-	27		104±9 ka	2-1024	MSA
Very Dark Greyish Brown 1,2,3	VDGB	-	6	845	96±5 ka	3-1056	MSA
Brown 3	-	28.5	-	989	91±6 ka	1-1023	MSA
Dark Yellowish Brown hearth	DYB	1	8	743			MSA
Dark Yellowish Brown	DYB	13.5	26	741, 580		-	MSA
MSA volumes		43	67				
Iron Age layers							
Grey	-	12.5	16	702, 691		-	Iron Age
Pinkish Grey	-	8	2	624, 603		-	Iron Age
Dark Reddish Grey pit	DRG	17	11	298, 296		-	Iron Age
E9 Dark Reddish Grey hearth 2 Plan 2–4	DRG hearth	-	4	300			Iron Age
D9 Dark Reddish Grey hearth 1 Plans 1–4	DRG hearth	32	6	351, 337, 158	250±80 yrs BP		Iron Age
Dark Reddish Grey Plans 2 & 3	DRG	10	5	514, 300			Iron Age
Dark Reddish Grey Plan 1	DRG	21	8	295, 282			Iron Age
Brown 2	-	4.5		388		-	Iron Age
Brown 1	-	10	3				Iron Age
Surface Plan 2	-	14	5			-	Iron Age
Surface Plan 1	-	6	20	11, 19			Iron Age
Iron Age volumes		135	80				
Total volume MSA and Iron Age		178	147				

TABLE 4

Number of individual K-feldspar grains measured, together with the number of grains rejected and accepted, and the reasons for their rejection. All grains that passed criteria 1–4 were used to construct the standardised growth curve (SGC). Rejection criteria 1–5: 1 = Initial T_n signal <3σ above corresponding background count, or relative standard error on T_n >25%; 2 = Recuperation ratio >5%; 3 = Figure-of-merit (FOM) value for L_x/T_x ratio >10%; 4 = Reduced-chi-square value for L_x/T_x ratios >5; 5 = D_e value obtained by extrapolation of dose-response curve beyond the largest regeneration dose, or L_n/T_n ratio statistically consistent with or higher than the saturation limit of the dose-response curve.

Sample	Method of measurement	No. of grains measured	Rejection criteria					Sum of grains rejected	No. of grains accepted
			1	2	3	4	5		
1-1023	SAR	500	403	27	30	2	4	466	34
1-1023 (residual)	SAR	300	244	38	9	0	0	291	9
1-1023 (dose recovery)	SGC	400	353					353	47
1-1023	SGC	1200	1100					1100	100
2-1024	SGC	1000	945					945	55
3-1056	SGC	1000	883					883	117

TABLE 5

Dose rate data, equivalent dose (D_e), overdispersion (OD) values, and ages for K-feldspar samples. [a] Beta, gamma and cosmic-ray dose rates were corrected for 5±1% water content. Measured water contents were 1.2–2.1%. [b] Total dose rate includes a cosmic-ray dose rate estimate of 0.10±0.02 Gy/ka. [c] N is the total number of grains passing all rejection criteria, n is the number of grains above the T_n threshold used in the age model to calculate final D_e. [d] Final D_e values were estimated using CAM after outliers were removed using nMAD. [e] The values shown in and outside the brackets are the overdispersion (OD) before and after applying nMAD.

Sample	External dose rate (Gy/ka)[a]		Internal dose rate (Gy/ka)	Total dose rate (Gy/ka)[b]	No of grains (n/N)[c]	D_e (Gy)[d]	OD (%)[e]	T_n threshold (cts/0.1 s)	Age (ka)
	Beta	Gamma							
1-1023	1.06±0.04	0.82±0.03	0.85±0.07	2.83±0.09		259±13	19 (42)	200	91.4±5.7
2-1024	1.22±0.04	1.02±0.04	0.85±0.07	3.19±0.09	44/55	331±26	20 (39)	0	103.7±8.9
3-1056	1.13±0.04	0.88±0.03	0.85±0.07	2.96±0.09	39/49	285±12	12 (37)	400	96.4±5.4

TABLE 6

Red Balloon Rock Shelter rock types of cores, retouched pieces and whole flakes >20 mm. FGBI = fine-grained basal igneous rock.

	Quartz	Quartzite	Jaspilite	Sandstone	Siltstone	FGBI	Rhyolite
cores	2	5			2	2	
bipolar cores	11	2	1				
core trimming flakes	2	10	2	1	1		1
cortical flakes	6	8		2	1		
miscellaneous flakes	4	3		7	3	1	
Levallois flakes	1	7	1		8		
blades		9			3		
points	5	1					1
scrapers	2				4	2	
denticulates		1	1				
other retouched tools	3	1			1	1	
TOTAL	**36**	**47**	**5**	**10**	**23**	**6**	**2**

TABLE 7

Red Balloon Rock Shelter frequencies of Middle Stone Age chips, chunks, flakes, blades and specular hematite.

chips <20 mm	chunks	core trimming flakes	whole flakes	Levallois flakes & points	cortical flakes	broken flakes	blades	broken blades	specular hematite	
									>10 mm	<10 mm
2773	87	45	348	43	97	446	45	113	166	204

TABLE 8

Red Balloon Rock Shelter frequencies of Middle Stone Age cores.

bipolar	Levallois	radial/ centripetal	adjacent platform	single platform	multiple platform	casual	TOTAL f cores
54	20	4	4	4	1	32	119

TABLE 9

Red Balloon Rock Shelter frequencies of Middle Stone Age retouched pieces

Scraper		Point		Other tools	
end	5	bifacial	4	backed tool	3
side	13	unifacial whole	5	notch	2
end/side	3	unifacial tip	5	chisel	1
scraper/adze	1			adze	2
broken	3			awl	2
				denticulate whole & broken	8
				broken tool	32

TABLE 10

Plant taxa identified from seed and fruit remains at Red Balloon Shelter. Binomials are from SANBI (2016) and common names are given in English and Afrikaans.

Scientific name	**Common name**	**Family name**
Apodytes dimidiata	white pear, wit-peer	Icacinaceae (white pear)
Arachis hypogaea	peanut (exotic)	Fabaceae (pea)
Asclepiad-type seed		Apocynaceae (oleander)
Asteraceae		(daisy)
Berchemia zeyheri	red ivory, rooi-ivoor	Rhamnaceae (buffalo-thorn, blinkblaar)
Bridelia mollis	velvet sweetberry, fluweel-soetbessie	Phyllanthaceae (potatobush)
Commiphora spp. (min. 2 species)	corkwood, kanniedood	Burseraceae (myrrh)
Cucurbitaceae		Cucumber, pumpkin, gourd
Erythrophysa transvaalensis	red balloon, rooiklapperbos	Sapindaceae (litchi)
Euclea sp.	guarri, gwarrie	Ebenaceae (ebony)
Grewia spp. (min. 2 species)	raisin, rosyntjiebos	Malvaceae (hibiscus)
Lannea edulis	grape lannea, wildedruif	Anacardiaceae (mango)
Mimusops zeyheri	moepel	Sapotaceae (milkwood)
Olea europea var. *cuspidata*	wild olive, olienhout	Oleaceae (olive)
Pappea capensis	jacket-plum, doppruim	Sapindaceae (litchi)
Poaceae		(grass)
Pseudolachnostylis maprouneifolia	kudu-berry, koedoe-bessie	Euphorbia (naboom)
Rubiaceae		(gardenia)
Sclerocarya birrea	marula, maroela	Anacardiaceae (mango)
Searsia sp.	karee	Anacardiaceae (mango)
cf. *Vangueria*	wild medlar, wildemispel	Rubiaceae (gardenia)
cf. *Syzygium*	water-berry, waterbessie	Myrtaceae (myrtle)
Vitex pooara	poora-berry, poerabessie	Lamiaceae (sage)
Ziziphus mucronata	buffalo thorn, blinkblaar-wag-'n-bietjie	Rhamnaceae (buffalo-thorn, blinkblaar)
Unidentified: Type 1 & Type 2		

TABLE 11

Red Balloon Rock Shelter ceramics from various facies recovered from the surface collection (sc) and excavation (ex)

	Jar	**Constricted jar**	**Bowl**	**Indeterminate**	**Total**
Happy Rest	3				3
Diamant	1				1
Eiland	11	1	1		13
Letsibogo	14	7	23		44
Undecorated **sc**	12	4	5		21
sc total	41	12	29		82
Undecorated **ex**	2			70	72
Total	43	12	29	70	154

TABLE 12

Red Balloon Rock Shelter ostrich eggshell, snail shell (maybe *Achatina* sp.) and possibly bone beads. A = *Achatina* or snail shell; B = possible bone; OES = ostrich eggshell; * = ostrich eggshell that has had its outer cortex removed.

Layer	Total station #	Whole bead OES	Whole bead *Achatina*	Whole bead bone	Broken bead	Drilled shell whole	Drilled shell broken	Roughout	Unfinished bead broken
Surface	11						1		
Dark Reddish Grey	208	1							
Dark Reddish Grey	233	1			1 A, 1 OES				
Dark Reddish Grey Plan 1	282					1			
Dark Reddish Grey	295	3	1						
Dark Reddish Grey	296	3					1		
Dark Reddish Grey	298		1					1 OES	
Dark Reddish Grey	329	1							
Dark Reddish Grey	351						3		
Grey hearth Plan 1	350						1		
Grey hearth Plan 2	413						1		
Grey hearth Plan 2	414		1				2		
Brown 2 Plan 1	388				1 OES				
Dark Yellowish Brown	491							1 OES	
Pinkish Grey	587	1(1*)							
Pinkish Grey	598	3 (2*)	1	1	1 B				
Pinkish Grey	603	1							
Pinkish Grey	624	1(1*)	4	2 (?)	3 OES (3*), 1 B				1 B (?)
Greyish Brown Ash	709	1							
TOTAL		**16 (4*)**	**8**	**3**	**1A, 5 OES (3*), 2 B**	**1**	**9**	**2 OES**	**1 B (?)**